Published in final edited form as:
J Immunol. 2014 September 1; 193(5): 2469–2482. doi:10.4049/jimmunol.1303370.

ADAM9 is a Novel Product of Polymorphonuclear Neutrophils: Regulation of Expression and Contributions to Extracellular Matrix Protein Degradation During Acute Lung Injury[#]

Robin Roychaudhuri, PhD[*,‖], **Anja H. Hergrueter, BA**[*,‖], **Francesca Polverino, MD**[*,†,‡], **Maria E. Laucho-Contreras, MD**[*], **Kushagra Gupta, MD**[*], **Niels Borregaard, MD, PhD**[§], and **Caroline A. Owen, MD, PhD**[*,†,¶]

[*]Division of Pulmonary and Critical Care Medicine, Brigham and Women's Hospital, and Harvard Medical School, 77 Avenue Louis Pasteur, Boston, MA, 02115

[†]The Lovelace Respiratory Research Institute Albuquerque, NM

[‡]Pulmonary Department, University of Parma, Parma, Italy

[§]The Granulocyte Research Laboratory, Department of Hematology, University of Copenhagen, Denmark

Abstract

A disintegrin and a metalloproteinase domain 9 (ADAM9**) is known to be expressed by monocytes and macrophages. Herein, we report that ADAM9 is also a product of human and murine polymorphonuclear neutrophils (PMNs). ADAM9 is not synthesized de novo by circulating PMNs. Rather, ADAM9 protein is stored in the gelatinase and specific granules and the secretory vesicles of human PMNs. Unstimulated PMNs express minimal quantities of surface ADAM9, but activation of PMNs with degranulating agonists rapidly (within 15 min) increases PMN surface ADAM9 levels. Human PMNs produce small quantities of soluble forms of ADAM9 (sADAM9). Surprisingly, ADAM9 degrades several extracellular matrix (ECM) proteins including fibronectin, entactin, laminin, and insoluble elastin as potently as MMP-9. However, ADAM9 does not degrade types I, III, or IV collagen, or denatured collagens in vitro. To determine whether Adam9 regulates PMN recruitment or ECM protein turnover during inflammatory responses, we compared wild type (WT) and *Adam9*$^{-/-}$ mice in bacterial lipopolysaccharide (LPS)- and bleomycin-mediated acute lung injury (ALI). Adam9 lung levels increase 10-fold during LPS-mediated ALI in WT mice (due to increases in leukocyte-derived

[#]**Grant support:** This work was supported by National Institutes of Health (NIH) grants HL063137, HL086814, and HL111835, R01AI111475, the BWH-LRRI consortium, the Flight Attendant Medical Research Institute grant CIA#123046, and the Danish Medical Research Council

[**]**Abbreviations used:** ADAM, a disintegrin and metalloproteinase domain; ALI, acute lung injury; ARDS, acute respiratory distress syndrome; BAL, bronchoalveolar lavage; BALF, BAL fluid; DAPI, 4′,6-diamidino-2-phenylindole; ECM, extracellular matrix; IT, intratracheal; KRP+G buffer, Krebs-Ringer-phosphate-glucose buffer; LF, lactoferrin; MMP, matrix metalloproteinase; MP, metalloproteinase; NE, neutrophil elastase; NGAL, neutrophil gelatinase-associated lipocalin NGAL; Pck, pancytokeratin; RIPA, radioimmunoprecipitation assay; TIMP, tissue inhibitor of metalloproteinase; WT, wild type.

[¶]Address for correspondence: Caroline A. Owen, MD, PhD, Division of Pulmonary and Critical Care Medicine, Brigham and Women's Hospital and Harvard Medical School, 77 Avenue Louis Pasteur, 855B Harvard Institutes of Medicine Building, Boston, MA 02115. Tel: 617-525-5408; Fax: 617-525-5413, cowen@rics.bwh.harvard.edu.
[‖]These authors contributed equally to this manuscript.

Adam9), but Adam9 does not regulate lung PMN (or macrophage) counts during ALI. Adam9 increases mortality, promotes lung injury, reduces lung compliance, and increases degradation of lung elastin during LPS- and/or bleomycin-mediated ALI. Adam9 does not regulate collagen accumulation in the bleomycin-treated lung. Thus, ADAM9 is expressed in an inducible fashion on PMN surfaces where it degrades some ECM proteins, and promotes alveolar-capillary barrier injury during ALI in mice.

INTRODUCTION

A disintegrin and metalloproteinase domain (ADAM) proteinases are a family of ~30 type I transmembrane proteins belonging to the zinc-dependent metalloproteinase (MP) super-family. They are characterized by a multi-domain structure that includes: 1) a pro domain which maintains the MP domain in a latent form; 2) a MP domain; 3) a disintegrin domain which binds integrins to regulate cell-cell or cell-matrix adhesion and/or migration; 4) a cysteine rich and an epidermal growth factor-like domain which may promote cell-cell fusion and/or regulate cell adhesion; 5) a transmembrane domain which anchors ADAMs to cell surfaces; and 6) a cytoplasmic tail which can participate in intracellular signaling (1,2).

ADAM9 (MDC-9/Meltrin-γ) is expressed by monocytes (3), activated macrophages (4), fibroblasts (5), epithelial cells (6), activated vascular smooth muscle cells (7), and keratinocytes (8). It is also upregulated in these cells during pathologic processes, and expressed by some tumor cells (9–12). ADAM9 is first synthesized as a precursor proenzyme (M_r ~110 kDa). It is then processed to an active form (M_r ~84 kDa) in the medial-golgi apparatus by a furin-like pro protein convertase which cleaves proADAM9 at a consensus cleavage sequence between the pro and MP domains (13). Human and murine ADAM9 share 82% sequence homology at the amino acid level (14).

Little is known about the activities of ADAM9 in regulating physiologic or pathologic processes. Most is known about the function of ADAM9's MP domain. ADAM9 is an active MP and has the characteristic consensus sequence (*HEXXHXXGXXH)* of MPs with three histidine residues binding the catalytically essential zinc atom in the catalytic domain. ADAM9's MP domain is not inhibited by tissue inhibitors of metalloproteinases [TIMPs (15)] and its physiologic inhibitors have not yet been identified. ADAM9's MP domain cleaves a limited number of extracellular proteins including: 1) the insulin B chain (16); 2) insulin-like growth factor binding proteins (17); 3) amyloid precursor protein at the α-secretase cleavage site in the non-amyloidgenic pathway (18); 4) ligands for the epidermal growth factor receptor from cell surfaces (19); and 5) fibroblast growth factor receptor 2iiib from tumor cell surfaces to contribute to tumor cell growth and metastasis (11). ADAM9's MP domain also contributes to the formation of multinucleate giant cells from monocytes and macrophages by mechanisms that are not clear (3). While there have been a small number of reports that a few ADAM proteinases cleave a limited number of extracellular matrix (ECM) proteins (20,21), it is not known whether ADAM9's MP domain cleaves ECM proteins to promote tissue remodeling or injury.

Less is known about the function of ADAM9's other domains. The disintegrin domain of ADAM9 binds to various integrins including: 1) α6β1 integrin to promote adhesion of

fibroblast cell lines (22); 2) α1, α3, α6, αv, and β1 integrins to regulate adhesion of human embryonic kidney-293 cells (23); and 3) β1 integrins on macrophages to promote macrophage fusion to form multinucleated giant cells in mycobacterial-induced granulomas (24). Both the disintegrin and cysteine rich domains of ADAM9 interact with the β1 integrin subunit on keratinocytes to promote keratinocyte migration (25). The cytoplasmic domain of ADAM9 binds protein kinase-C δ isoform to promote shedding of heparin-binding epidermal grown factor from cell surfaces (26).

Although ADAM9 is expressed by monocytes and macrophages, it is not known whether ADAM9 is expressed by PMNs and, if so, whether it regulates PMN function or contributes to pericellular proteolysis and tissue injury. Neither Adam9's expression in the lung during acute lung injury (ALI) nor its activities in regulating ALI have been investigated previously. To begin to address these knowledge gaps, we assessed whether ADAM9 is expressed by PMNs, characterized the forms of ADAM9 that are produced by PMNs, and assessed the biology of ADAM9 in PMNs. We assessed whether PMN-derived ADAM9 contributes to PMN pericellular proteolysis of ECM proteins in vitro. We also compared WT and *Adam9*$^{-/-}$ mice in murine models of acute neutrophilic lung inflammation and injury to determine whether Adam9 regulates PMN accumulation in the lung, injury to the lung, and/or ECM protein turnover during ALI syndromes.

MATERIALS AND METHODS

Materials

Recombinant human ADAM9 ectodomain and the human ADAM9 ELISA kit were purchased from R&D Systems (Minneapolis, MN). Rabbit anti-ADAM9 IgG (Ab36176) and murine anti-pancytokeratin IgG and antibodies to PMN granule markers were purchased from Abcam (Cambridge, MA). Rat anti-murine Ly6G and rat anti-murine Mac-3 IgGs were purchased from BD Pharmingen (San Jose, CA). Purified human pro-matrix metalloproteinase-8 (proMMP-8) and proMMP–9 were purchased from Chemicon International, Inc. (Temecula, CA). DQ®-FITC-conjugated gelatin, DQ®-FITC-conjugated type IV collagen, DQ®-FITC-conjugated type I collagen, and goat anti-rabbit F(ab')$_2$ conjugated to Alexa-488 (GAR-Alexa-488) were purchased from Invitrogen (Carlsbad, CA). FITC-conjugated particulate elastin (MESH 200–400) was purchased from ICN Biomedicals Inc (Aurora, OH). L-α-phosphatidylcholine-β-y-O-alkyl platelet activating factor (PAF) was purchased from Bachem (Torrence, CA). Optimized ADAM9 and 18S Taqman® primer and probe sets were purchased from Ambion (Austin, TX). Vectashield mounting medium with DAPI was purchased from Vector Laboratories (Burlingame, CA). The murine desmosine ELISA kit was purchase from Antibodies-Online Inc. (Atlanta, GA). All other reagents were purchased from Sigma-Aldrich (St. Louis, MO).

Mice

The Harvard Medical School Animal Care and Use Committee approved all procedures performed on mice. C57BL/6 strain *Adam9*$^{-/-}$ mice were provided by Carl Blobel, MD, PhD (Hospital for Special Surgery, New York, NY). Age- and gender-matched adult C57BL/6 WT mice (8–12 weeks of age) were purchased from The Jackson laboratory (Bar

Harbor, ME) and studied as experimental controls. The genotype of the *Adam9*$^{-/-}$ mice was determined using PCR-based genotyping protocols conducted on genomic DNA extracted from murine tail biopsies.

Isolation of human PMNs

All human subject studies were approved by the Partners Healthcare Institutional Review Board. Human PMNs (>95% pure and >99% viable) were isolated from the peripheral blood of healthy human volunteers using the ficoll-Hypaque method (27).

Activation of PMNs

Human PMNs (10^7/ml in PBS) were incubated for 30 min at 37°C with or without PMA (0.3 μM), calcium ionophore (A23187; 1 μM), fMLP (10^{-6}–10^{-11} M), IL-8 (10^{-7}–10^{-10} M) or TNF-α (10^{-7} to 10^{-10} M). Other aliquots of cells were incubated with or without fMLP (10^{-7} M) or TNF-α (10^{-7} M) or IL-8 (10^{-7} M) at 37°C for up to 120 min. To test whether agonists have synergistic or additive effects on regulating surface ADAM9 levels on PMNs, we incubated human PMNs at 37°C for 15 min with or without optimal concentrations of bacterial LPS from E coli 0111B4 (100 ng/ml), PAF (10^{-7} M), or TNF-α (10^{-7} M), followed by the optimal concentration of fMLP (10^{-7} M) for 30 min at 37°C. Cells were then fixed for 5 min at 4°C in PBS containing 3% (wt/vol) paraformaldehyde and 0.5% (vol/vol) glutaraldehyde (pH 7.4), washed in PBS, and then immunostained for surface ADAM9, as outlined below.

Isolation and activation of murine PMNs

PMNs (>85% pure and >99% viable) were isolated from the bone marrow of *Adam9*$^{-/-}$ or WT mice by positive selection for Ly6G using immunomagnetic beads (28). Murine PMNs were incubated without agonists for 45 min or incubated with 10^{-6} M platelet-activating factor (PAF) or 10^{-6} M fMLP for 30 min at 37°C, or incubated at 37°C for 15 min with 10^{-6} M PAF followed by 10^{-6} M fMLP for 30 min. PMNs were fixed and washed (as described above), and then immunostained for surface Adam9 or used in cell-based proteolysis assays as outlined below.

Immunofluorescence staining for surface Adam9 protein levels

Unstimulated or activated human or murine PMNs were incubated at 4°C for 2 h in PBS containing 1% albumin and 50 μg/ml of goat IgG to block binding of antibodies to PMN Fc receptors. Cells were then incubated for 2 h at 4°C with rabbit anti-ADAM9 IgG or non-immune rabbit IgG (both at 1 μg/10^6 cells). The cells were washed twice in PBS and incubated for 2 h at 4°C with 4 μg/ml goat anti-rabbit F(ab')$_2$ conjugated to Alexa 488. The cells were washed twice in PBS, and cytocentrifuge preparations examined using either a confocal microscope or bright field and epifluorescence microscopy (Eclipse E-800, Nikon, Japan). For quantitative analysis of surface ADAM9 staining, images of the immunostained cells were captured using a Leica DFC480 camera (Leica Microsystems Ltd., Buffalo Grove, IL), and Adam9 staining was measuring using MetaMorph® software (Universal Imaging, West Chester, PA) exactly as described previously for other proteinases expressed on PMN surfaces (29).

Double immunostaining of permeabilized PMNs for ADAM9 and markers of PMN granules

Unstimulated human PMNs were permeabilized by incubating them in 100% methanol for 30 min at 4°C and then incubated overnight at 4°C in PBS containing 1% albumin, 10% normal goat serum, and 50 μg/ml goat IgG (for cells incubated with primary antibodies raised in mice) or 1% albumin, 10% normal mouse serum, and 50 μg/ml murine IgG (for cells incubated with primary antibodies raised in goats) to block non-specific binding of antibodies. Cells were then incubated with rabbit anti-ADAM9 IgG (or non-immune rabbit IgG) followed by goat anti-rabbit $F(ab')_2$ conjugated to Alexa 488 as outlined above. ADAM9 labeled cells were then washed and incubated with either murine anti-myeloperoxidase (MPO) IgG, murine anti-lactoferrin IgG, or goat anti-MMP-9 IgG (or non-immune murine or goat IgG as controls). Cells were then washed in PBS and incubated with goat anti-murine $F(ab')_2$ conjugated to Alexa 546 or rabbit anti-goat $F(ab')_2$ conjugated to Alexa 546. Nuclei were counterstained with 4′,6-diamidino-2-phenylindole (DAPI) and cells were then examined using a confocal microscope.

Subcellular fractionation of PMNs

Fresh buffy coats were obtained from the central blood bank at Rigshospitalet, Denmark. Dextran 500 solution (Sigma-Aldrich; 500 ml) was added to induce sedimentation of the red cells. The leukocyte-rich supernatant was layered on Lymphoprep (Axix-Schield PoC AS, Oslo, Norway) and centrifuged. Contaminating red cells were lysed by hypotonic shock as described previously (30). The PMNs were resuspended at 3×10^7 cells/ml in Krebs-Ringer-phosphate-glucose (KRP+G buffer; pH 7.4) and split in two equal aliquots. One aliquot was incubated at 4 °C (unstimulated), the other was incubated at 37°C for 5 min and then PMA (2–5 μg/ml) was added. After 15 min, equal volumes of ice-cold KRP+G buffer were added to both samples. The cells were centrifuged and the supernatant fluids (S_0) were frozen to −80°C for analysis. The cells were resuspended at 3×10^7 cells/ml in KRP+G buffer containing diisopropyl fluorophosphate (Calbiochem, Darmstadt, Germany), centrifuged and resuspended in 12.5 ml relaxation buffer (31), and subjected to nitrogen cavitation (30).

The post-nuclear supernatant was subjected to fractionation on a three-layer Percoll density gradient which efficiently separates the organelles into fractions enriched in azurophil granules (α-band, identified by MPO); specific granules (β1-band, identified by neutrophil gelatinase-associated lipocalin [NGAL]); gelatinase granules [β2-band, identified by MMP-9]), and a fraction rich in both the secretory vesicles (identified by albumin) and the plasma membranes (identified by HLA) (32). Fractions (1 ml total of each) were aspirated and those with peak MPO concentrations (fractions #1–8), peak NGAL concentrations (fractions #9–14), peak MMP-9 concentrations (fractions #15–19), and peak albumin and HLA concentrations (#20–28) were pooled. Percoll was removed by ultracentrifugation and the biological material collected and resuspended in 1 ml of PBS as described previously (30,31). Fractions #29–40 (S_2) containing the cytosol were also collected. Subcellular fractionates (azurophil, specific, and gelatinase granules along with the plasma membrane and secretory vesicle faction were solubilized by incubating them with an equal volume of radioimmunoprecipitation assay (RIPA) buffer (50 mM Tris buffer containing 150 mM NaCl, 1% Triton X-100, 0.1% deoxycholate, 0.1% SDS, 100 mM PMSF, and 100 mM 1,10 o-phenanthroline). Proteins in the fractions along with the cytosol were separated on 12%

SDS-PAGE, and them immunoblotted for ADAM9 using rabbit anti-ADAM9 IgG (Abcam), goat anti-rabbit IgG conjugated to horseradish peroxidase, and an enhanced chemiluminescence (ECL) plus detection system (Pierce, Rockford, IL). ADAM9 was quantified in solubilized granules and vesicles, and also the cytosolic and cell-free supernatant samples using a commercial ELISA and ADAM9 levels were normalized to total protein levels using a commercial kit (Biorad, Hercules, CA).

Quantitative real time (RT)-RT-PCR to measure ADAM9 steady state mRNA levels in PMNs

Human PMNs (24 x 10^6 cells per assay) were activated at 37°C for 15 min with 10^{-7} M TNF-α followed by 10^{-7} M fMLP for up to 4 h. RNA was isolated from the cells using an RNeasy kit (Qiagen Corp., Valencia, CA), and RNA concentration and purity was measured using a Nanodrop Spectrophotometer 2000 device (Thermo Scientific, Waltham, MA). RNA samples (500 ng) were reverse transcribed using Moloney Murine Leukemia Virus Reverse Transcriptase, reverse transcriptase buffer, deoxyribonucleotide triphosphate mixture, and γ-RNase inhibitor. We used Taqman® gene expression probes and primer sets for human ADAM9 and 18S as the housekeeping gene (Applied Biosystems/Invitrogen, Grand Island, NY). Samples were amplified using a Stratagene MxPro-Mx3005P real time PCR system (Stratagene, La Jolla CA).

Analysis of ADAM9 levels and forms in PMNs

Human PMNs (20 x 10^6/ml) were incubated in PBS with or without 10^{-7} M fMLP for up to 2 h at 37°C and then PMNs and cell-free supernatant samples were separated by centrifugation (500 g for 5 min). PMN were washed once in PBS and PMN extracts prepared at 10^7 cells/ml in RIPA containing 100 mM PMSF, and 100 mM 1,10 o-phenanthroline. ADAM9 was quantified in cell extracts (from 0.5 million cells/experimental condition) and cell-free supernatant samples using a commercial ELISA kit. ADAM9 forms in these samples were assessed by Western blot analysis as outlined above.

Effects of proteinase inhibitors on PMN production of soluble ADAM9 (sADAM9 forms)

To determine whether sADAM9 forms produced by PMNs are generated by proteolytic shedding from the PMN surface, we incubated human PMNs (20 x 10^6/ml) with or without 10^{-7} M fMLP or PMA (200 nM) in the presence and absence of the following inhibitors: 1) 4-(2-aminoethyl)benzenesulfonyl fluoride (100 μM), a serine proteinase inhibitor; 2) GM6001 (50 μM), a general inhibitor of metalloproteinases; 3) pepstatin A (50 μM), an inhibitor of aspartic acid proteinases; and 4) leupeptin (50 μM) an inhibitor of cysteine proteinases; or 5) E64 (50 μM) an inhibitor of cysteine proteinases. After 2 h, cell-free supernatant fluids were harvested, and sADAM9 levels were measured using an ELISA. Results of sADAM9 levels produced by PMNs incubated with proteinase inhibitors were expressed as a percentage of the sADAM9 levels produced by PMNs in the absence of inhibitors.

Binding of exogenous ADAM9 ectodomain to the PMN surface

To determine whether ADAM9's ectodomain can bind to the plasma membrane of PMNs, we incubated PMNs (2 x 10^6/assay in 100 μl of PBS) with or without 1 or 2 μM recombinant

ADAM9 ectodomain for 2 h at 4°C. Unbound ADAM9 was removed by washing the cells twice with PBS. PMNs were then fixed and immunostained for ADAM9 as outlined above.

Active-site titration of human ADAM9, MMP-9, MMP-8, and neutrophil elastase (NE)

Purified human proMMP-9 and proMMP-8 were activated by incubation for 3 h at 37°C with 1 mM 4-amino-phenylmercuric acetate (APMA) and active-site titrated using human tissue inhibitor of metalloproteinase-2 (TIMP-2) as described previously (28,33,34).

We confirmed that our rADAM9 preparation was pure by demonstrating a single band corresponding to the size of the ectodomain (~60 kDa) when we analyzed rADAM9 on silver stained 12% SDS-PAGE gels. We also detected no contaminating MMP-8 or -9 when we performed Western blotting for MMP-8 or MMP-9 on rADAM9 that had been subjected to electrophoresis on 12% SDS-PAGE gels. We used RS113456, a general hydroxamate inhibitor of metalloproteinases, to active-site titrate ADAM9. Briefly, 100 nM of ADAM9 was incubated for 30 min at 37°C with or without 0.5–250 nM RS113456, and then 10 μM Mca-4-yl acetyl P-L-A-Q-A-V-(3–2,4 DNP-L-2, 3 DAP)-R-S-S-S-R-NH_2 [a quenched fluorogenic peptide substrate containing the sequence in pro-TNF-α that is cleaved by ADAM17 and ADAM9 (15)] was added and samples incubated at 37°C. Cleavage of this substrate was measured over 18 h using fluorimetry (Hitachi F2500 fluorescence spectro-fluorimeter, Tokyo, Japan) using Ex λ 320 and Em λ 405. Substrate cleavage was plotted against the concentration of RS113456 tested and the concentration of active ADAM9 was determined by regression analysis using SigmaPlot (Jandel Scientific Software, San Jose, CA). Human NE was active site titrated as described previously (35).

Cleavage of ECM proteins by soluble rADAM9 vs. soluble MMPs

We incubated equimolar amounts (2 μM) of active-site titrated ADAM9 (or MMP-9 or MMP-8 or buffer alone as controls) for 18 h at 37°C with 2 μg of type I collagen, laminin, fibronectin, or entactin, or 20 μg of type III collagen in 20–50 μl of Tris assay buffer (50 mM Tris containing 150 mM NaCl and 20 mM $CaCl_2$; pH 7.4) containing 0.05 % Triton X-100. The reaction was terminated by adding 10 μl of 3X SDS sample buffer (50 mM Tris HCl containing 100 mM DTT, 2% SDS, 0.1% bromophenol blue and 10% glycerol; pH 6.8) and heating the samples at 100°C for 10 min. ADAM9 (25 nM) or buffer alone were also incubated with fibronectin (2 μg) for 2, 4, 8, and 18 h at pH 7.4. The reaction mixtures were separated on 4–20% Tris-glycine SDS gradient electrophoresis gels (Bio-Rad Laboratories, Hercules, CA) and proteins were stained with Coomassie Blue R-250. We used Scion Image software (Scion Corporation, Frederick, MD) to quantify the intensities of the bands of residual intact substrate and calculated the percentage of the substrate that was cleaved by each proteinase in 3–4 separate experiments.

For ECM proteins that are commercially available in quenched FITC-conjugated forms, we incubated 25 nM of active MMP-9, MMP-8, or ADAM9, or buffer alone in 200 μl of Tris assay buffer (at pH 7.4) with 50 μg/ml quenched DQ®-FITC-conjugated gelatin, quenched DQ®-FITC-conjugated type IV collagen, or quenched DQ®-FITC-conjugated type I collagen at 37°C for 18 h. Cleavage of the substrates was quantified using fluorimetry (excitation λ 495 nm and emission λ 520 nm). To quantify cleavage of elastin, equimolar

amounts (25 nM) of active-site titrated ADAM9, MMP-8, MMP-9, or human neutrophil elastase (NE), or buffer alone were incubated at 37°C in 200 μl Tris assay buffer with 20 mg/ml elastin-FITC, and elastin cleavage was quantified at intervals in aliquots of eluates using fluorimetry (28).

Cleavage of ECM by membrane bound Adam9 on PMNs

We used a loss-of-function strategy to determine whether membrane-bound Adam9 expressed on the surface of activated murine PMNs has the same spectrum of catalytic activity as soluble ADAM9 ectodomain by comparing the surface MP-mediated proteolytic activity associated with equal numbers of activated PMNs from WT versus *Adam9*$^{-/-}$ mice or Mmp-8 or -9 deficient mice as controls. We and other investigators have previously validated similar cell-based assay systems to quantify the contributions of MMPs and other ADAM proteinases to proteolytic events occurring on cell surfaces (28,34,36,37).

WT, *Adam9*$^{-/-}$, *Mmp-9*$^{-/-}$, and *Mmp-8*$^{-/-}$ PMNs were optimally activated with 10^{-6}M PAF for 15 min followed by 10^{-6} M fMLP for 30 min to induce surface expression of Adam9, Mmp-8 (34), and Mmp-9 (28) on WT cells. Cells were then fixed as described above to prevent release of soluble proteinases during the assays (28,34) and resuspended in Tris assay buffer (0.05M Tris containing 0.15 M NaCl and 0.02 M Ca Cl_2; pH 7.4). Equal numbers of cells from each genotype were incubated in triplicate at 37°C for 30 min with 1 mM PMSF to completely inactivate cell surface serine proteinases on PMNs which contribute to cleavage of the substrates studied (28,34,35,38,39). Samples were divided into two equal aliquots, and one aliquot was incubated for 30 min at 37°C with 1 mM 1,10 o-phenanthroline [a general inhibitor of MMPs and ADAM proteinases (28,40)], and the other aliquot was incubated without this inhibitor. PMNs or buffer alone were then incubated for 18 h at 37°C with 50 μg/ml DQ-FITC-conjugated type IV collagen (3 x 10^6 cells/assay), DQ-FITC-conjugated gelatin (3 x10^6 cells/assay), DQ-FITC-conjugated type I collagen (5 x10^6 cells/assay), or 20 mg/ml FITC-conjugated particulate elastin (Mesh 200–400; 5 x10^6 cells/assay) in Tris assay buffer (pH 7.4). We measured the MP-mediated cell surface activity associated with *Adam9*$^{-/-}$, *Mmp-8*$^{-/-}$, *Mmp-9*$^{-/-}$ and WT PMNs as the 1,10 o-phenanthroline-inhibitable cleavage of each substrate. The MP activity associated with the surface of proteinase-deficient PMNs was expressed as a percentage of the activity that was associated with equal numbers of WT PMNs in 4–6 separate experiments.

LPS-mediated ALI in mice

WT and *Adam9*$^{-/-}$ mice were anesthetized with i.p. injections of ketamine (100 mg/kg), xylazine (10 mg/kg), and acepromazine (3 mg/kg). LPS from *E Coli* 0111:B4 (10 μg in 30 μl of endotoxin-free PBS) or 30 μl of endotoxin-free PBS alone were delivered to WT and *Adam9*$^{-/-}$ mice by the intra-tracheal (IT) route to induce robust PMN accumulation in the lungs of C57BL/6 WT mice (34,41).

Adam-9, -10, and -17 steady state mRNA levels in the lungs of mice during LPS-mediated ALI

Lungs were removed from mice 4 and 24 h after delivering LPS or PBS by the IT route. RNA was extracted from the lungs using Trizol reagent and an RNeasy kit (42), and RNA

samples were reverse transcribed as described above. We used a SYBR-green protocol to amplify the samples using the following primers: Adam9 forward primer: 5′-GCG CTG TGT GGA AAG CTT C-3′; Adam9 reverse primer: 5′-AAA CAC CGG CAT GTC CTG TAC-3′; GAPDH forward primer: 5′-CCAGGAAAT GAGCTTGAGAAAGT-3′; Adam10 forward primer: 5′-TTG CCG CCT CCT AAA CCA C-3′; Adam10 reverse primer: 5′-TGG CGG TCT CCT CCT CTT T-3′; Adam17 forward primer: 5′-AGT GGC AGG ACT TCT TCA GTG G-3′; Adam17 reverse primer: 5′-CCC TAG AFT CAG GCT CAC CAA C-3′; GAPDH reverse primer: 5′-CCCACTCCTCCAC CTTTGAC-3′. Fold change in Adam gene expression was quantified using the $\Delta\Delta C_T$ method and GAPDH as the housekeeping control gene.

Immunofluorescence staining for Adam9 in lung sections

We performed immunoperoxidase staining on inflated and formalin-fixed lung sections obtained from WT mice 24 h after LPS was instilled by the IT route (41) or lung sections from unchallenged WT mice using rabbit anti-Adam9 IgG (Ab36176) or non-immune rabbit IgG as a control. To identify the cell types in the lung that express Adam9 during ALI, we double immunostained lung sections obtained from unchallenged WT mice or WT mice 24 h after LPS was instilled for Adam9 and markers of leukocyte subsets or lung epithelial cells. Sections from formalin-fixed lungs were subjected to antigen retrieval by heating them at 100°C in 0.01 M sodium citrate and 2 mM citric acid buffer for 10 min. Lungs were then incubated with rabbit anti-Adam9 IgG or non-immune rabbit IgG for 2 h at 37°C followed by goat anti-rabbit $F(ab')_2$ conjugated to Alexa-488. Lung sections were then incubated for 1 h at 37°C with either rat anti-murine Mac-3 IgG (to identify macrophages), rat anti-murine Ly6G IgG (to identify PMNs), or murine anti-pancytokeratin IgG (to identify epithelial cells). Lungs were washed again in PBS and incubated for 1 h at 37°C with goat anti-rat $F(ab')_2$ conjugated to Alexa 546 or goat anti-murine $F(ab')_2$ conjugated to Alexa 546. Lungs were incubated in 2.2 mM Sudan Black dye in 70% ethanol for 25 min at room temperature, mounted in Vectashield Mounting Medium containing DAPI, and coverslips were applied. Immunostained lung sections were then examined using a confocal microscope.

Activities of Adam9 in LPS-mediated acute lung inflammation and lung injury in mice

At intervals after inducing ALI, mice were euthanized, bronchoalveolar lavage (BAL) was performed, and total and differential leukocytes were counted in BAL samples (41). To assess whether Adam9 regulates lung injury in mice, we measured total protein and hemoglobin levels in BAL samples and quantified wet-to-dry lung weight ratios, as described previously (41).

Activities of Adam9 in regulating bleomycin-mediated ALI and collagen accumulation in the lungs of mice

WT and *Adam9*$^{-/-}$ mice were anesthetized with i.p. injections of ketamine (100 mg/kg) xylazine (10 mg/kg), and acepromazine (3 mg/kg) and 30–100 mU of bleomycin in 30 μl of endotoxin-free saline or 30 μl of saline alone was delivered to WT vs. *Adam9*$^{-/-}$ mice by the IT route. In one cohort of mice, weight loss and mortality was monitored over 21 days. Other cohorts of mice were euthanized at intervals over 10 days and BAL was performed.

Absolute numbers of PMN, macrophages, monocytes, and lymphocytes were counted in BAL samples 3, 7, and 10 days after instilling bleomycin.

In other cohorts of mice, respiratory mechanics (lung elastance, lung resistance, and quasi-static compliance) were measured on anesthetized and tracheostomized mice using a digitally-controlled mechanical ventilator (FlexiVent device; SCIREQ, Inc., Montreal, Quebec, Canada) 7 days after instilling 100 mU of bleomycin or saline, exactly as described previously (41). Wet-to-dry lung weight ratios were also measured after euthanizing the animals.

Collagen deposition in the lung was measured 21 days after delivering bleomycin or saline by measuring hydroxyproline levels in hydrolysates of left lungs and staining formalin-fixed right lung sections with Masson's trichrome stain, as described previously (42).

Statistical Analysis

Data are expressed as mean ± SEM or mean ± SD. The results for paired and unpaired data were compared using the Mann-Whitney rank sum test for non-parametric data using Sigmastat. P values less than 0.05 were considered significant.

RESULTS

ADAM9 is expressed in an inducible manner on the surface of human and murine PMNs

To determine whether ADAM9 is expressed by PMNs, we immunostained non-permeabilized unstimulated and fMLP-activated human PMNs with a green fluorophore for surface ADAM9 and examined the cells using a confocal microscope. Unstimulated PMNs expressed minimal quantities of ADAM9 on their surface. However, fMLP induced robust expression of ADAM9 on the surface of PMNs (Fig. 1A).

To quantify the effects of agonists on surface ADAM9 levels on PMNs, we incubated human PMNs for varying times with varying concentrations of pharmacologic and biologically-relevant agonists and quantified surface ADAM9 levels. Pharmacologic agonists that robustly induce PMN degranulation (PMA and A23187) induced striking increases in surface ADAM9 levels on PMNs within 30 min (Fig. 1B). Pro-inflammatory agonists that also promote PMN degranulation (fMLP, IL-8, and TNF-α) induced concentration-dependent increases in surface ADAM9 levels on PMNs (Figs. 1C, 1D, and 1E, respectively). The effect of these mediators was also rapid. Significant increases in surface ADAM9 levels were detected within 5–15 min of adding fMLP (Fig. 1F), TNF-α (Supplemental Fig. 1), or IL-8 (Supplemental Fig. 2) to PMNs. Surface ADAM9 levels returned to or below baseline levels after incubating PMNs with agonists for 120 min. Pro-inflammatory mediators induced additive increases in surface ADAM9 levels on PMNs as surface ADAM9 levels were higher on PMNs activated with LPS, PAF, or TNF-α followed by fMLP when compared with cells incubated with optimal concentrations of each agonist alone (Fig. 1G). Pro-inflammatory mediators also rapidly increased surface Adam9 levels on PMNs isolated from unchallenged WT mice (Fig.1H).

ADAM9 is not synthesized de novo by PMNs

We used real time RT-PCR to determine whether ADAM9 expression is regulated at the steady state mRNA level in activated human PMNs. Although we detected transcripts for a housekeeping gene (18 S) in PMNs (mean C_T = 23.95 ± SD 0.45 for unstimulated PMN versus C_T =25.56 ± 0.47 for PMNs activated for 4 h with 10^{-7}M fMLP), we did not detect ADAM9 transcripts in either unstimulated or fMLP-activated PMNs (no cycle detected for any experimental condition using the ADAM9 primer and probe sets).

When we measured total ADAM9 protein levels in extracts of unstimulated human PMNs using an ELISA, we detected ~66 pg of ADAM9/million cells, but ADAM9 protein levels did not change significantly when cells were activated with pro-inflammatory agonists for 30 min (Table I), 1–4 h (Table II) or 6 h (data not shown). Thus, PMNs do not synthesize ADAM9 *de novo*.

ADAM9 is stored in the tertiary and specific granules and also in the secretory vesicles of human PMNs

As serine proteinases and MMPs are stored within different PMN granules (2) and translocate to the PMN surface when cells undergo degranulation (28,29,34,39), we tested whether this is the case for ADAM9. We double immunostained methanol-permeabilized, unstimulated human PMNs for intracellular ADAM9 and markers of the three types of granules present in PMNs: the azurophil (using myeloperoxidase [MPO] as a marker), specific (using lactoferrin [LF] as a marker), and the tertiary or gelatinase granules (using MMP-9 as a marker). These studies localized ADAM9 mainly to the tertiary granules of PMNs as intense co-localization of ADAM9 and MMP-9 was detected using confocal microscopy (Fig. 2A). Co-localization of ADAM9 and the specific granule marker, lactoferrin, was also detected (Fig. 2A). However, ADAM9 was not detected in the MPO-containing PMN azurophil granules. Cells stained with isotype-matched non-immune primary antibodies showed minimal or no staining (Fig. 2A).

We also subjected unstimulated and PMA-activated human PMNs to subcellular fractionation as described in Methods. When the PMN granule fractions, and the fraction containing both the plasma membrane and secretory vesicles were detergent-solubilized and subjected to immuno-blotting for ADAM9, a single band of this proteinase was detected in the tertiary (or gelatinase) granules and to a lesser extent in specific granules in unstimulated PMNs but no signal was present in the azurophil granule fraction (Fig. 2B, top panel). The intensity of the ADAM9 band present in the tertiary and specific granules of PMA-stimulated cells (Fig. 2B, lower panel) was lower than that in the same granule fractions in unstimulated PMNs. The latter result is consistent with PMA-triggered degranulation and translocation of these granules (and their complement of ADAM9) to the plasma membrane. However, the most intense ADAM9 signal in unstimulated PMNs was detected in the fraction containing both the plasma membranes and secretory vesicles of PMNs (the MV fraction). Secretory vesicles are present in segmented PMNs and undergo exocytosis. Secretory vesicles contain plasma proteins suggesting that they are formed by (in part) by endocytosis (43,44). This MV fraction contained a second higher molecular mass form of ADAM9. Both ADAM9 signals in the MV fraction decreased in intensity (albeit more

modestly than the ADAM9 signals in the gelatinase and specific granules) when PMNs were activated with PMA. Several faint ADAM9 bands were detected in the cytosol faction of unstimulated PMNs. The form having the same M_r as that detected in the granule and MV fractions was not present in the cytosol fraction of PMA-activated PMNs. We confirmed these findings when we quantified ADAM9 protein levels in the solubilized granule and MV fractions using an ELISA (Fig. 2C).

Together, these results indicate that mature PMNs store ADAM9 protein in their tertiary and specific granules, and that substantial quantities of ADAM9 are also present in the combined plasma membrane and secretory vesicle fraction of PMNs. Moreover, activation of PMNs results in a redistribution of ADAM9 with translocation of ADAM9 from the tertiary and specific granules and the secretory vesicles to the PMN surface.

PMNs produce several soluble forms of ADAM

Western analysis of PMN supernatant samples revealed that human PMNs produce several forms of soluble ADAM9 (sADAM9). Two main sADAM9 forms (M_r ~87 and ~78 kDa) were detected in cell-free supernatant fluids from PMNs incubated without agonists for 60 min (data not shown). When fMLP-activated PMNs produced additional sADAM9 forms including a major form having a M_r ~75 kDa and a less abundant form having a M_r ~56 kDa (data not shown). When we quantified sADAM9 levels in cell-free supernatant samples from PMNs using an ELISA, the total amount of sADAM9 released by the cells did not change significantly when cells were activated (Tables I and II).

To assess whether sADAM9 forms are generated by proteolytic shedding of ADAM9 ectodomain from PMN surfaces, we incubated PMNs with or without fMLP, and with or without inhibitors of serine proteinases (AEBSF), metalloproteinases (GM6001), aspartic acid proteinases (pepstatin A) and cysteine proteinases (leupeptin or E64). None of these inhibitors, either when tested separately or together, blocked the generation of sADAM9 by PMNs under either basal or stimulated conditions (data not shown). Thus, sADAM9 forms are not generated by proteolytic shedding of ADAM9's ectodomain from the PMN surface.

Soluble ADAM9 can bind to the PMN surface

Other soluble proteinases expressed by PMNs including serine proteinases and MMPs can bind to the external surface of the plasma membrane of PMNs following their release by PMNs (28,29,34,39). To test whether this is also the case for sADAM9, we incubated PMNs with or without exogenous sADAM9 ectodomain at 4°C, removed unbound protein by washing the cells, and then measured surface ADAM9 levels by immunostaining. The results show that sADAM9 can bind to the PMN plasma membrane but only when relatively high concentrations (2 μM) are present in extracellular fluids (Supplemental Fig. 3).

Soluble ADAM9 ectodomain degrades ECM protein

Activated PMNs are associated with potent pericellular proteolytic activity when they adhere to and migrate on ECM proteins (45,46). To determine whether ADAM9 contributes to PMN pericellular proteolysis, we tested the activity of purified recombinant human ADAM9 (rADAM9) ectodomain against basement membrane proteins and structural ECM

proteins (including insoluble elastin and interstitial collagens) at physiologic pH (7.4). To estimate the efficiency of ADAM9 as an ECM protein-degrading proteinase, we also compared its activities to those of equimolar amounts of soluble MMP-8 and MMP-9. We chose these MMPs as controls because, like ADAM9, they are produced by PMNs and expressed on the surface of activated PMNs where they contribute to PMN-mediated pericellular proteolysis (28,34). MMP-8 potently degrades interstitial collagens and some basement membrane proteins (34), whereas MMP-9 degrades denatured collagen (gelatin), elastin, and many basement membrane proteins (28). Preliminary experiments confirmed that neither MMP-8 nor -9 were present (as contaminants) in our rADAM9 preparation as assessed by Western blot analysis (data not shown).

Basement membrane proteins—Soluble human rADAM9 degrades fibronectin, entactin, and laminin (Fig. 3). ADAM9 was modestly but significantly more efficient at degrading fibronectin than MMP-9 but less potent than MMP-8 (Fig. 3A). When tested against entactin, ADAM9 was ~3-fold more efficient than MMP-9 and had similar potency as MMP-8 (Fig. 3B). ADAM9 was only slightly less efficient than MMP-9 at degrading laminin (Fig. 3C). However, unlike MMP-9 or neutrophil elastase (NE, a serine proteinase which is also expressed by PMNs), ADAM9 was not a type IV collagenase (Fig. 3D) even when a high concentration (up to 2 μM) of ADAM9 was tested. When we assessed the time course for ADAM9-mediated degradation of one basement membrane protein (fibronectin), ADAM9 progressively degraded this substrate over 18 h, and significant degradation of this protein occurred as early as 2 h after adding ADAM9 (Fig. 3E).

Structural components of the ECM—Soluble human ADAM9 had no detectable activity against type I collagen (Fig. 3F) or type III collagen (data not shown). Unlike MMP-9, ADAM9 also had no activity against denatured type I collagen (gelatin; Fig. 3G). Surprisingly, ADAM9 degraded particulate insoluble elastin and was as potent at degrading insoluble elastin as MMP-9 (Fig. 3H). Both MMP-9 and ADAM9 were only one third as potent as NE at degrading insoluble elastin (Fig. 3H). When we assessed the time course for ADAM9-mediated degradation of elastin, ADAM9 progressively degraded this substrate over 18 h. Significant degradation of this protein was detected as early as 2 h after adding ADAM9 (Supplemental Fig. 4).

Together, these data indicate that ADAM9 is an ECM protein-degrading proteinase. Moreover, ADAM9 has a unique spectrum of catalytic activity degrading some basement membrane components and elastin (like MMP-9). However, ADAM9 has no activity against gelatin or basement membrane collagen (unlike MMP-9) and no activity against type I or III interstitial collagens (unlike MMP-8).

Membrane-bound ADAM9 degrades a similar spectrum of ECM proteins as soluble ADAM9

ADAM9 is a transmembrane proteinase, and most (~95%) of the ADAM9 that is expressed by PMNs is cell-associated (Tables I and II). Thus, we tested whether membrane-bound ADAM9 has a similar spectrum of activity as sADAM9 ectodomain against ECM proteins. To accomplish this, we used a published loss-of-function strategy that we and others have used to assess the contributions of MMPs and other ADAM proteinases expressed on cell

surfaces to pericellular proteolysis that is associated with intact cells (28,34,36,37). We compared the surface metalloproteinase activities associated with equal numbers of activated PMNs isolated from WT mice versus mice deficient in individual proteinases against ECM substrates found to be susceptible (elastin) or not susceptible (type I collagen and gelatin) to cleavage by soluble sADAM9 (see Fig. 3). Unlike membrane-bound Mmp-8 on activated PMNs, membrane-bound Adam9 had no detectable type I collagenase activity (Fig. 4A). Unlike membrane-bound Mmp-9 on activated PMNs, membrane-bound Adam9 had no gelatinase activity (Fig. 4B). However, membrane-bound Adam9 degraded particulate elastin as potently as membrane-bound Mmp-9 on activated PMNs (Fig. 4C). Thus, both soluble and membrane bound ADAM9 have significant elastase but not interstitial collagenase or gelatinase activities.

Activities of Adam9 in regulating PMN accumulation and lung ECM protein degradation during ALI in mice

During ALI or its more severe form, the acute respiratory distress syndrome (ARDS), there is robust recruitment of PMNs to the lung and PMN-derived proteinases contribute to lung injury (47). Degradation of lung ECM proteins by PMN-derived proteinases contributes significantly to alveolar capillary barrier injury, lung edema, and mortality during ALI in human subjects and experimental animals (48–53). Levels of an elastin degradation product (desmosine) are increased in urine and/or lung samples from human ALI/ARDS patients and animals with ALI, and levels correlate positively with lung injury and mortality (53,54). It is not known whether the MP or disintegrin domains of PMN-derived Adam9 regulate PMN trans-endothelial migration and PMN recruitment into inflamed tissues. It is also not known whether the MP domain of PMN-derived ADAM9 contributes to PMN proteolysis of ECM proteins and tissue injury during inflammatory responses in the lung. To begin to address these knowledge gaps, we compared WT and *Adam9*$^{-/-}$ mice in murine models of neutrophilic lung inflammation (IT instillation of LPS or bleomycin) and quantified Adam9 expression, PMN accumulation in the lungs, lung injury, and turnover of two ECM proteins, one which is sensitive (elastin) and one which is resistant (type I collagen) to ADAM9 degradation in vitro (see Figs. 3 and 4).

Adam9 is up-regulated in the lungs of mice with ALI

After IT instillation of LPS in C57BL/6 WT mice, we measured steady state Adam9 mRNA levels in whole lung samples using qRT-RT-PCR. Adam9 steady state mRNA lung levels increased 10-fold 4 h after delivering IT LPS to WT mice, and Adam9 levels returned to baseline after 24 h (Fig. 5A). In contrast, no significant changes in Adam10 or Adam17 steady state mRNA levels were detected in lung samples 4 or 24 h after instillation of LPS.

Immunoperoxidase staining of lung sections from unchallenged vs. LPS-treated WT mice showed minimal staining for Adam9 in the lungs of unchallenged mice, but robust staining for Adam9 in the lungs 24 h after delivering LPS mainly in leukocytes recruited to the lungs (Fig. 5B). To identify the cells in which Adam9 expression is increased in the lung, we double immunostained lung sections for Adam9 and markers of leukocyte subsets (Ly6G for PMNs and Mac-3 for macrophages) and lung epithelial cells (pancytokeratin). There was minimal staining for ADAM9 in resident lung macrophages or lung epithelial cells in

unchallenged WT mice (Fig. 5C). In contrast, intense staining for ADAM9 was detected in lung macrophages and PMNs recruited to the lungs of LPS-treated WT mice (Fig. 5D). Positive staining for Adam9 was also detected in bronchial epithelial cells in LPS-treated WT mice (Fig. 5D), but there was minimal staining for Adam9 in alveolar epithelial cells (data not shown).

ADAM9 is not required for PMN accumulation in the lung during LPS- or bleomycin-mediated ALI

To assess whether Adam9 regulates the accumulation of PMNs (or macrophages) following lung injury, we compared PMN and macrophage counts in BAL samples from LPS-treated WT and *Adam9*$^{-/-}$ mice. WT and *Adam9*$^{-/-}$ mice did not differ in BAL total leukocyte counts (Fig. 6A), PMN counts (Fig. 6B), or macrophage counts (data not shown) at any time point from 4 h to 7 days after IT LPS. BAL PMN and macrophage counts did not differ 3 or 7 days after IT instillation of 30 mU of bleomycin (data not shown).

ADAM9 promotes lung injury and proteolysis of lung elastin in mice with LPS-mediated ALI

When compared with WT mice, *Adam9*$^{-/-}$ mice were significantly protected from lung injury following instillation of LPS as assessed by measuring: 1) wet-to-dry lung weight ratios (Fig. 6C); 2) BAL fluid (BALF) total protein levels (Fig. 6D); and 3) BAL hemoglobin levels (a marker of leakage of erythrocytes across the alveolar-capillary barrier; Fig. 6E). To assess whether Adam9 degrades lung elastin during ALI to contribute to alveolar capillary barrier injury, we measured BALF desmosine levels in WT and *Adam9*$^{-/-}$ mice with LPS-mediated ALI. LPS increased BALF desmosine levels in WT mice, but LPS-treated *Adam9*$^{-/-}$ mice had significantly lower BALF desmosine levels than LPS-treated WT mice (Fig. 6F).

Adam9 promotes lung injury but does not regulate lung fibro-proliferative responses during bleomycin-induced ALI

Saline-treated WT and *Adam9*$^{-/-}$ mice did not lose weight, and all of the saline-treated mice survived as expected (Fig. 7A and 7B). However, compared with bleomycin-treated WT mice, bleomycin-treated *Adam9*$^{-/-}$ mice lost less body weight (Fig. 7A) and had higher survival rates (~80% survival versus ~50% survival; Fig 7B). When compared with WT mice, *Adam9*$^{-/-}$ mice were protected from bleomycin-mediated ALI as assessed by measuring weight-to-dry lung weight ratios 7 days after delivering bleomycin or saline (Fig. 7C). To further assess ALI, we measured respiratory mechanics on WT and *Adam9*$^{-/-}$ mice 7 days after they were treated with bleomycin or saline. Bleomycin-treated *Adam9*$^{-/-}$ mice had significantly lower increases in lung elastance (a measure of lung stiffness; Fig 7D) and lower reductions in quasi-static lung compliance (Fig. 7E) indicating that *Adam9*$^{-/-}$ mice have less severe bleomycin-mediated ALI than WT mice. The lower weight loss and higher survival rates in the bleomycin-treated *Adam9*$^{-/-}$ mice likely reflect the less severe ALI in these animals when compared with bleomycin-treated WT mice.

As Adam9 does not degrade interstitial collagens or denatured collagens in vitro (see Fig. 3 and 4), we next assessed whether Adam9 regulates collagen accumulation in the lung

following IT instillation of bleomycin. WT and *Adam9*$^{-/-}$ mice had similar lung fibroproliferative responses to bleomycin as assessed by hematoxylin and eosin staining (data not shown) and Masson's Trichrome staining of lung sections from the mice (Fig. 7F). WT and *Adam9*$^{-/-}$ mice also had similar lung collagen levels 21 days after instilling bleomycin as assessed by hydroxyproline assays performed on lung hydrolysates (Fig. 7G). Thus, Adam9 does not regulate collagen accumulation in the lung after instillation of bleomycin.

DISCUSSION

To our knowledge, this is the first report that ADAM9 is expressed by both human and murine PMNs. PMNs produce both transmembrane and sADAM9 forms, but transmembrane-bound ADAM9 is the most abundant (>90%) form produced by PMNs. ADAM9 is not synthesized de novo by circulating PMNs. Rather, ADAM9 protein is stored in PMN tertiary and specific granules. Substantial quantities are also detected in the combined secretory vesicle and plasma membrane fraction of PMNs. Moreover, ADAM9 translocates to the PMN surface from these granules and vesicles when PMNs degranulate. Surprisingly, ADAM9 degrades some basement membrane proteins and insoluble elastin, but has no type IV or interstitial collagenase activity in vitro. We also provide novel insights into the expression and activities of ADAM9 during ALI by showing that ADAM9 levels are robustly upregulated in lung PMNs (and lung macrophages) during ALI in mice, but Adam9 is not required for PMN (or macrophage) accumulation in the lungs of mice with ALI. Adam9 promotes lung injury, mortality, and lung elastin degradation during ALI. However, Adam9 does not regulate lung collagen deposition following IT instillation of bleomycin. Thus, ADAM9 is a novel PMN product that contributes to PMN extracellular proteolysis. Adam9 promotes ALI in mice and this may be mediated, in part, by Adam9 degrading lung elastin (and possibly basement membrane proteins) in the lung.

Biology of ADAM9 in PMNs

ADAM9 has not been studied previously in leukocytes other than monocytes and macrophages (3,24). While ADAM9 is regulated at the transcriptional level in monocytes and macrophages (3,10,55), ADAM9 is not regulated at the mRNA level in mature PMNs. ADAM9 is likely transcribed by PMN precursors in the bone marrow and stored as a performed proteinase within PMN granules and vesicles. ADAM9 is redistributed to the PMN surface when PMNs are activated by pro-inflammatory mediators as is the case for PMN-derived serine proteinases and MMPs (2). ADAM8 and ADAM17 are the only other members of the ADAM family known to be expressed by primary PMNs (56–58) but ADAM10 is expressed by PMN-like HL60 cells (59). However, little is known about the biology of ADAM10 or ADAM17 in PMNs.

PMN products other than ADAM9 are also localized in more than one granule in PMNs. For example, ADAM8 is localized mainly in the tertiary and specific granules and to a lesser extent in azurophil granules (58), CD11b/CD18 is also stored in all three PMN granules, the fMLP receptor and SNAP 23–25 are stored in the specific and gelatinase granules, and lysozyme is detected in the azurophil and gelatinase granules (60). ADAM9 may be distributed to different PMN compartments during granule biogenesis during the maturation

of myeloid precursor cells in the bone marrow. PMN granules are formed sequentially during the differentiation of myeloid cells in the bone marrow. The MPO-rich azurophil granules form first during the early promyelocyte stage, and this is followed by the appearance of the lactoferrin-rich specific granules at the myelocyte and metamyelocyte stages. The MMP-9-rich tertiary granules form next during the band cells and segmented PMNs stages, and lastly the secretory vesicles (which also undergo exocytosis) appear during the segmented PMN stage (60). These granules and vesicles are packaged with proteins that are synthesized at the same time during granulopoiesis. The known heterogeneity in PMN granule protein content is thus due to differences in the biosynthetic windows of individual granule proteins which, in turn, reflects different patterns of transcription factors present at distinct stages of myeloid cell development (61).

Although little is know about the transcription factors that regulate the expression of ADAM9 in PMNs, likely the transcription factors involved are mostly activated during the later myelocyte to segmented PMNs stages to explain the partitioning of ADAM9 into the gelatinase granules and secretory vesicles and, to a lesser extent, the specific granules. It is noteworthy that we detected large quantities of ADAM9 in the combined plasma membrane and secretory vesicle fraction in unstimulated PMNs and the ADAM9 signal in this fraction decreased when cells were activated with PMA. The latter result supports our conclusion that ADAM9 is also stored within the secretory vesicles as our immunostaining results show that: 1) minimal amounts of ADAM9 are associated with the plasma membrane of unstimulated PMNs; and 2) the amount of ADAM9 in the plasma membrane strikingly increases when cells are activated with PMA. Also, the secretory vesicles contain plasma proteins (such as albumin), which suggests that they are formed by endocytosis as well as granulopoiesis. Thus, ADAM9 that translocates to the surface of PMNs via fusion of the tertiary and specific granules with the PMN's plasma membrane may subsequently be endocytosed from the plasma membrane into the secretory vesicles. This possibility might explain (in part) the large quantities of ADAM9 that we detected in the combined plasma membrane and secretory vesicle fraction both in unstimulated and PMA-activated PMNs. The localization of ADAM9 in PMN tertiary granules and secretory vesicles is consistent with the very rapid (within 5 min) increases in surface ADAM9 levels on PMNs after adding agonists, as both storage compartments are known to translocate to the PMN plasma membrane more rapidly than the more dense azurophil granules (45).

PMNs produce small amounts of sADAM9 forms, but these are not generated via proteolytic shedding of transmembrane-bound ADAM9 from the PMN surface, as we could not block their generation by incubating PMNs with synthetic inhibitors of all four classes or proteinases. It is possible that ADAM9 forms lacking the transmembrane domain are also stored within PMN granules and freely released by the cells during PMNs degranulation. Some tumor cells produce sADAM9 forms having biologic activities (62). However, to our knowledge, PMNs are the only non-malignant cell type that produces sADAM9. Whether PMN-derived sADAM9 forms contribute to ADAM9's activities in vivo is not clear. However, it is noteworthy that the amount of sADAM9 generated by PMNs is small relative to the total amount which is expressed by the cells (~5%). Likely, transmembrane-bound ADAM9 is the main form contributing to ADAM9's activities in vivo. Although our results showed that sADAM9 ectodomain can bind to the external surface of the PMN plasma

membrane, this occurs only when PMNs are incubated with high concentrations of sADAM9 (2 μM). As we detected only relatively low concentrations of sADAM9 in cell-free supernatant fluids from both unstimulated and activated PMNs (Tables I and II and Fig. 2C), it is unlikely that binding of sADAM9 contributes significantly to the pericellular proteolytic activity that is associated with activated PMNs unless PMNs are present in tissues in very high numbers such as in abscesses. Rather, our results indicate that most of the surface-bound ADAM9 that we detected on the surface of activated PMNs is the result of translocation of ADAM9 from intracellular storage sites rather than sADAM9 that is released from the cells binding to the plasma membrane.

ECM protein-degrading activities of ADAM9

ADAM proteins are closely related to snake venom proteinases which can degrade basement membrane (type IV) collagen. However, until now, there has been little evidence that ADAMs are significant ECM-degrading proteinases (2). While ADAM10 has type IV-collagenase activity, this activity is very modest in magnitude (63). ADAM9's ectodomain and PMN-derived transmembrane Adam9 both potently degrade several ECM proteins. Surprisingly, ADAM9 was as potent as MMP-9 in degrading insoluble elastin, and as potent (or more potent) than MMP-9 in degrading several basement membrane proteins.

Among MP family members, ADAM9's spectrum of catalytic activity most resembles that of MMP-9 (28,45) as elastin, fibronectin, laminin, and entactin were susceptible to cleavage by both proteinases. However, ADAM9 had no activity against basement membrane (type IV) collagen or gelatin (denatured collagen), both of which are degraded by MMP-9. Adam9 is a significant elastase in vivo as LPS-treated *Adam9*$^{-/-}$ mice had substantially reduced BALF levels of desmosine (an elastin-degradation product), which were associated with less severe ALI when compared with LPS-treated WT mice. Adam9 did not increase lung elastin degradation or promote lung injury by increasing inflammatory cell burdens in the lung as LPS- and bleomycin-treated WT and *Adam9*$^{-/-}$ mice had similar lung PMN and macrophage counts. Thus, while NE is a more potent elastase than ADAM9 on a molar basis in vitro, Adam9 may have more potent elastin-degrading activities in the murine lung than either NE or MMP-9 as neither neutrophil elastase-deficient nor Mmp9-deficient mice are protected from LPS-mediated ALI (64,65). As expected, ADAM9 had no activity in vitro against interstitial collagens present in the lung (types I and III), and Adam9 did not regulate type I collagen accumulation in the lungs following bleomycin instillation in mice suggesting that it is not an interstitial collagenase in the lung.

A prior study reported that ADAM9 has ECM protein-degrading activities, as sADAM9 released by tumor cells degrades laminin (62). Our study adds to the literature by more fully characterizing the ECM protein-degrading profile of sADAM9 and comparing its efficiency to that of equimolar amounts of other key ECM protein degrading proteinases that are expressed by PMNs. We also assessed the ECM- degrading activities of transmembrane-bound Adam9 by murine PMNs.

ADAM9 expression and activities during lung inflammation

Adam9 has not been studied previously in animal models of ALI. Adam9 gene expression increased in the lung during LPS-mediated ALI. Immunostaining studies showed that increases in lung Adam9 levels during ALI were due to the recruitment of PMNs to the lungs, and increased expression of Adam9 by lung macrophages and to a lesser extent by bronchial epithelial cells. Likely, the increased steady state mRNA levels detected in whole lung samples reflected increased Adam9 gene expression in lung macrophages and epithelial cells. We showed that Adam9 was not essential for PMNs (or macrophages) to accumulate in the lungs during LPS- or bleomycin-mediated ALI in mice suggesting that neither the MP nor the disintegrin domain of PMN or monocytes/macrophage-derived ADAM9 regulate inflammatory cell recruitment into the lung. In contrast, the MP domains of PMN-derived Adam-8 and -17 regulate inflammatory responses in tissues by shedding L-selectin, TNF-α, and TNF receptors from PMN surfaces (66–68). During LPS- and bleomycin-mediated ALI, Adam9 promoted lung injury and reduced lung compliance without altering lung inflammatory cell counts in mice. Adam9 also increased weight loss and mortality in bleomycin-treated mice which likely reflected the more severe ALI in mice expressing Adam9.

Strengths and limitations of this study

Strengths of our manuscript include our comprehensive analysis of the biology of ADAM9 in PMNs. We identified an unexpected function for ADAM9 ectodomain (ECM protein degradation) and compared the relative activities of ADAM9 in this respect to those of other key proteinases expressed by PMNs. We confirmed that: 1) transmembrane-bound Adam9 on intact PMNs has elastin-degrading activities; 2) Adam9 has significant elastin-degrading (but not collagenase) activity in the lungs of mice with ALI; and 3) Adam9 promotes lung injury in two models of neutrophilic lung inflammation in mice. We also showed that PMNs recruited to the lungs of mice are a significant source of Adam9 in the lung using immunostaining methods.

A limitation of our study is that we focused our in vivo studies on only one ECM protein that is sensitive (elastin) or resistant (type I collagen) to ADAM9-mediated cleavage in vitro as we currently lack reliable methods for assessing proteolysis of basement membrane proteins that are susceptible to cleavage by ADAM9 in lung injury model systems. Additionally, we did not determine whether ADAM9 promotes ALI in mice by cleaving proteins other than ECM proteins in the lung. These topics are beyond the scope of the current manuscript, but will be investigated in our future studies as appropriate tools become available.

Clinical relevance

Our results have clinical relevance as proteolysis of ECM proteins occurs in the lung during ALI. Levels of protein fragments of elastin and other ECM proteins are increased in BALF, plasma, and urine samples from ALI/ARDS patients, and levels correlate positively with lung injury and mortality (48–53,69). Proteolytic degradation of lung ECM proteins contributes to ALI pathogenesis by causing loss of epithelial cell-ECM attachments, alveolar epithelial cell anoikis, and alveolar edema (47,70,71). Our results suggest that ADAM9

contributes significantly to this process. Strategies that inhibit the activity of ADAM9's MP domain, or reduce its expression or half life in the lung could reduce alveolar capillary barrier injury, and thereby reduce the high morbidity and mortality that is associated with ALI/ARDS.

Conclusions

ADAM9 is a novel product of PMNs that is rapidly mobilized to the extracellular space when PMNs are activated. ADAM9 contributes significantly to PMN pericellular proteolysis and elastin degradation in vitro. ADAM9 expression is upregulated in the lung during neutrophilic ALI in mice and contributes to lung elastin degradation and alveolar capillary barrier injury in mice, but does not regulate inflammatory cell recruitment in the lung. Thus, ADAM9 is a novel PMN product that promotes ALI in mice.

Supplementary Material

Refer to Web version on PubMed Central for supplementary material.

References

1. Blobel CP. ADAMs: key components in EGFR signalling and development. Nat Rev Mol Cell Biol. 2005; 6:32–43. [PubMed: 15688065]
2. Owen CA. Leukocyte cell surface proteinases: regulation of expression, functions, and mechanisms of surface localization. Int J Biochem Cell Biol. 2008; 40:1246–1272. [PubMed: 18329945]
3. Namba K, Nishio M, Mori K, Miyamoto N, Tsurudome M, Ito M, Kawano M, Uchida A, Ito Y. Involvement of ADAM9 in multinucleated giant cell formation of blood monocytes. Cell Immunol. 2001; 213:104–113. [PubMed: 11831872]
4. Izumi Y, Hirata M, Hasuwa H, Iwamoto R, Umata T, Miyado K, Tamai Y, Kurisaki T, Sehara-Fujisawa A, Ohno S, Mekada E. A metalloprotease-disintegrin, MDC9/meltrin-gamma/ADAM9 and PKCdelta are involved in TPA-induced ectodomain shedding of membrane-anchored heparin-binding EGF-like growth factor. EMBO J. 1998; 17:7260–7272. [PubMed: 9857183]
5. Zigrino P, Nischt R, Mauch C. The disintegrin-like and cysteine-rich domains of ADAM-9 mediate interactions between melanoma cells and fibroblasts. J Biol Chem. 2011; 286:6801–6807. [PubMed: 21135106]
6. Mahimkar RM, Visaya O, Pollock AS, Lovett DH. The disintegrin domain of ADAM9: a ligand for multiple beta1 renal integrins. Biochem J. 2005; 385:461–468. [PubMed: 15361064]
7. Al Fakhri N, Wilhelm J, Hahn M, Heidt M, Hehrlein FW, Endisch AM, Hupp T, Cherian SM, Bobryshev YV, Lord RS, Katz N. Increased expression of disintegrin-metalloproteinases ADAM-15 and ADAM-9 following upregulation of integrins alpha5beta1 and alphavbeta3 in atherosclerosis. J Cell Biochem. 2003; 89:808–823. [PubMed: 12858346]
8. Mauch C, Zamek J, Abety AN, Grimberg G, Fox JW, Zigrino P. Accelerated wound repair in ADAM-9 knockout animals. J Invest Dermatol. 2010; 130:2120–2130. [PubMed: 20376065]
9. Oksala N, Levula M, Airla N, Pelto-Huikko M, Ortiz RM, Jarvinen O, Salenius JP, Ozsait B, Komurcu-Bayrak E, Erginel-Unaltuna N, Huovila AP, Kytomaki L, Soini JT, Kahonen M, Karhunen PJ, Laaksonen R, Lehtimaki T. ADAM-9, ADAM-15, and ADAM-17 are upregulated in macrophages in advanced human atherosclerotic plaques in aorta and carotid and femoral arteries--Tampere vascular study. Ann Med. 2009; 41:279–290. [PubMed: 19253070]
10. Dehmel T, Janke A, Hartung HP, Goebel HH, Wiendl H, Kieseier BC. The cell-specific expression of metalloproteinase-disintegrins (ADAMs) in inflammatory myopathies. Neurobiol Dis. 2007; 25:665–674. [PubMed: 17207628]
11. Peduto L V, Reuter E, Shaffer DR, Scher HI, Blobel CP. Critical function for ADAM9 in mouse prostate cancer. Cancer Res. 2005; 65:9312–9319. [PubMed: 16230393]

12. Peduto L. ADAM9 as a potential target molecule in cancer. Curr Pharm Des. 2009; 15:2282–2287. [PubMed: 19601830]
13. Roghani M, Becherer JD, Moss ML, Atherton RE, Erdjument-Bromage H, Arribas J, Blackburn RK, Weskamp G, Tempst P, Blobel CP. Metalloprotease-disintegrin MDC9: Intracellular maturation and catalytic activity. J Biol Chem. 1999; 274:3531–3540. [PubMed: 9920899]
14. Weskamp G, Kratzschmar J, Reid MS, Blobel CP. MDC9, a widely expressed cellular disintegrin containing cytoplasmic SH3 ligand domains. J Cell Biol. 1996; 132:717–726. [PubMed: 8647900]
15. Amour A, Knight CG, English WR, Webster A, Slocombe PM, Knauper V, Docherty AJ, Becherer JD, Blobel CP, Murphy G. The enzymatic activity of ADAM8 and ADAM9 is not regulated by TIMPs. FEBS Lett. 2002; 524:154–158. [PubMed: 12135759]
16. Roghani M, Becherer JD, Moss ML, Atherton RE, Erdjument-Bromage H, Arribas J, Blackburn RK, Weskamp G, Tempst P, Blobel CP. Metalloprotease-disintegrin MDC9: intracellular maturation and catalytic activity. J Biol Chem. 1999; 274:3531–3540. [PubMed: 9920899]
17. Mohan S, Thompson GR, Amaar YG, Hathaway G, Tschesche H, Baylink DJ. ADAM-9 is an insulin-like growth factor binding protein-5 protease produced and secreted by human osteoblasts. Biochemistry. 2002; 41:15394–15403. [PubMed: 12484779]
18. Allinson TM, Parkin ET, Turner AJ, Hooper NM. ADAMs family members as amyloid precursor protein alpha-secretases. J Neurosci Res. 2003; 74:342–352. [PubMed: 14598310]
19. Dang M, Dubbin K, D'Aiello A, Hartmann M, Lodish H, Herrlich A. Epidermal growth factor (EGF) ligand release by substrate-specific a disintegrin and metalloproteases (ADAMs) involves different protein kinase C (PKC) isoenzymes depending on the stimulus. J Biol Chem. 2011; 286:17704–17713. [PubMed: 21454702]
20. Martin J, Eynstone LV, Davies M, Williams JD, Steadman R. The role of ADAM 15 in glomerular mesangial cell migration. J Biol Chem. 2002; 277:33683–33689. [PubMed: 12091380]
21. Black RA, White JM. ADAMs: focus on the protease domain. Curr Opin Cell Biol. 1998; 10:654–659. [PubMed: 9818177]
22. Nath D, Slocombe PM, Webster A, Stephens PE, Docherty AJ, Murphy G. Meltrin gamma (ADAM-9) mediates cellular adhesion through alpha(6)beta(1)integrin, leading to a marked induction of fibroblast cell motility. J Cell Sci. 2000; 113(Pt 12):2319–2328. [PubMed: 10825303]
23. Mahimkar RM, Visaya O, Pollock AS, Lovett DH. The disintegrin domain of ADAM9: a ligand for multiple beta1 renal integrins. Biochem J. 2005; 385:461–468. [PubMed: 15361064]
24. Puissegur MP, Lay G, Gilleron M, Botella L, Nigou J, Marrakchi H, Mari B, Duteyrat JL, Guerardel Y, Kremer L, Barbry P, Puzo G, Altare F. Mycobacterial lipomannan induces granuloma macrophage fusion via a TLR2-dependent, ADAM9- and beta1 integrin-mediated pathway. J Immunol. 2007; 178:3161–3169. [PubMed: 17312164]
25. Zigrino P, Steiger J, Fox JW, Loffek S, Schild A, Nischt R, Mauch C. Role of ADAM-9 disintegrin-cysteine-rich domains in human keratinocyte migration. J Biol Chem. 2007; 282:30785–30793. [PubMed: 17704059]
26. Izumi Y, Hirata M, Hasuwa H, Iwamoto R, Umata T, Miyado K, Tamai Y, Kurisaki T, Sehara-Fujisawa A, Ohno S, Mekada E. A metalloprotease-disintegrin, MDC9/meltrin-gamma/ADAM9 and PKCdelta are involved in TPA-induced ectodomain shedding of membrane-anchored heparin-binding EGF-like growth factor. EMBO J. 1998; 17:7260–7272. [PubMed: 9857183]
27. Boyum A. Isolation of mononuclear cells and granulocytes from human blood: Isolation of mononuclear cells by one centrifugation and of granulocytes by combining centrifugation and sedimentation at 1 g. Scand J Clin Lab Invest. 1963; 21(Suppl 97):77–89.
28. Owen CA, Hu Z, Barrick B, Shapiro SD. Inducible expression of tissue inhibitor of metalloproteinases-resistant matrix metalloproteinase-9 on the cell surface of neutrophils. Am J Resp Cell Mol Biol. 2003; 29:283–294.
29. Owen CA, Campbell MA, Sannes PL, Boukedes SS, Campbell EJ. Cell-surface-bound elastase and cathepsin G on human neutrophils. A novel, non-oxidative mechanism by which neutrophils focus and preserve catalytic activity of serine proteinases. J Cell Biol. 1995; 131:775–789. [PubMed: 7593196]

30. Borregaard N, Heiple JM, Simons ER, Clark RA. Subcellular localization of the b-cytochrome component of the human neutrophil microbicidal oxidase: translocation during activation. J Cell Biol. 1983; 97:52–61. [PubMed: 6408102]

31. Clemmensen SN, Udby L, Borregaard N. Subcellular fractionation of human neutrophils and analysis of subcellular markers. Methods Mol Biol. 2014; 1124:53–76. [PubMed: 24504946]

32. Kjeldsen L, Sengelov H, Lollike K, Nielsen MH, Borregaard N. Isolation and characterization of gelatinase granules from human neutrophils. Blood. 1994; 83:1640–1649. [PubMed: 8123855]

33. O'Connell JP, Willenbrock F, Docherty AJP, Eaton D, Murphy G. Analysis of the role of the COOH-terminal domain in the activation, proteolytic activity, and tissue inhibitor of metalloproteinase interactions of gelatinase B. J Biol Chem. 1994; 269:14967–14973. [PubMed: 8195131]

34. Owen CA, Hu Z, Lopez-Otin C, Shapiro SD. Membrane-bound matrix metalloproteinase-8 on activated polymorphonuclear cells is a potent, tissue inhibitor of metalloproteinase-resistant collagenase and serpinase. J Immunol. 2004; 172:7791–7803. [PubMed: 15187163]

35. Owen CA, Campbell MA, Boukedes SS, Campbell EJ. Cytokines regulate membrane-bound leukocyte elastase on neutrophils: A novel mechanism for effector activity. Am J Physiol (Lung Cell Mol Physiol). 1997; 272:L385–L393.

36. Weskamp G, Ford JW, Sturgill J, Martin S, Docherty AJ, Swendeman S, Broadway N, Hartmann D, Saftig P, Umland S, Sehara-Fujisawa A, Black RA, Ludwig A, Becherer JD, Conrad DH, Blobel CP. ADAM10 is a principal 'sheddase' of the low-affinity immunoglobulin E receptor CD23. Nat Immunol. 2006; 7:1293–1298. [PubMed: 17072319]

37. Sahin U, Weskamp G, Kelly K, Zhou HM, Higashiyama S, Peschon J, Hartmann D, Saftig P, Blobel CP. Distinct roles for ADAM10 and ADAM17 in ectodomain shedding of six EGFR ligands. J Cell Biol. 2004; 164:769–779. [PubMed: 14993236]

38. Owen CA, Campbell MA, Boukedes SS, Campbell EJ. Inducible binding of cathepsin G to the cell surface of neutrophils: A mechanism for mediating extracellular proteolytic activity of cathepsin G. J Immunol. 1995; 155:5803–5810. [PubMed: 7499869]

39. Campbell EJ, Campbell MA, Owen CA. Bioactive proteinase 3 on the cell surface of human neutrophils: quantification, catalytic activity, and susceptibility to inhibition. J Immunol. 2000; 165:3366–3374. [PubMed: 10975855]

40. Knolle MD, Nakajima T, Hergrueter A, Gupta K, Polverino F, Craig VJ, Fyfe SE, Zahid M, Permaul P, Cernadas M, Montano G, Tesfaigzi Y, Sholl L, Kobzik L, Israel E, Owen CA. Adam8 limits the development of allergic airway inflammation in Mice. J Immunol. 2013; 190:6434–6449. [PubMed: 23670189]

41. Quintero PA, Knolle MD, Cala LF, Zhuang Y, Owen CA. Matrix metalloproteinase-8 inactivates macrophage inflammatory protein-1 alpha to reduce acute lung inflammation and injury in mice. J Immunol. 2010; 184:1575–1588. [PubMed: 20042585]

42. Enari M, Hug H, Nagata S. Involvement of an ICE-like protease in Fas-mediated apoptosis. Nature. 1995; 375:78–81. [PubMed: 7536900]

43. Cowland JB, Borregaard N. The individual regulation of granule protein mRNA levels during neutrophil maturation explains the heterogeneity of neutrophil granules. J Leukoc Biol. 1999; 66:989–995. [PubMed: 10614782]

44. Borregaard N, Miller LJ, Springer TA. Chemoattractant-regulated mobilization of a novel intracellular compartment in human neutrophils. Science. 1987; 237:1204–1206. [PubMed: 3629236]

45. Owen CA, Campbell EJ. The cell biology of leukocyte-mediated proteolysis. J Leukoc Biol. 1999; 65:137–150. [PubMed: 10088596]

46. Owen CA, Campbell EJ. Extracellular proteolysis: new paradigms for an old paradox. J Lab Clin Med. 1999; 134:341–351. [PubMed: 10521080]

47. Owen, CA.; Campbell, EJ. Proteinases. In: Haslett, C.; Evans, T., editors. ARDS: Acute Respiratory Distress in Adults. 1. Chapman & Hall Medical; London: 1996. p. 139-165.

48. Kawamura M, Yamasawa F, Ishizaka A, Kato R, Kikuchi K, Kobayashi K, Aoki T, Sakamaki F, Hasegawa N, Kawashiro T, Ishihara T. Serum concentration of 7S collagen and prognosis in

patients with the adult respiratory distress syndrome. Thorax. 1994; 49:144–146. [PubMed: 8128404]

49. Kondoh Y, Taniguchi H, Taki F, Takagi K, Satake T. 7S collagen in bronchoalveolar lavage fluid of patients with adult respiratory distress syndrome. Chest. 1992; 101:1091–1094. [PubMed: 1555426]
50. Kropf J, Grobe E, Knoch M, Lammers M, Gressner AM, Lennartz H. The prognostic value of extracellular matrix component concentrations in serum during treatment of adult respiratory distress syndrome with extracorporeal CO2 removal. Eur J Clin Chem Clin Biochem. 1991; 29:805–812. [PubMed: 1797106]
51. Chesnutt AN, Matthay MA, Tibayan FA, Clark JG. Early detection of type III procollagen peptide in acute lung injury. Pathogenetic and prognostic significance. Am J Respir Crit Care Med. 1997; 156:840–845. [PubMed: 9310002]
52. Adamson IY, King GM, Bowden DH. Collagen breakdown during acute lung injury. Thorax. 1988; 43:562–568. [PubMed: 2463695]
53. McClintock DE, Starcher B, Eisner MD, Thompson BT, Hayden DL, Church GD, Matthay MA. Higher urine desmosine levels are associated with mortality in patients with acute lung injury. Am J Physiol Lung Cell Mol Physiol. 2006; 291:L566–L571. [PubMed: 16698854]
54. Tenholder MF, Rajagopal KR, Phillips YY, Dillard TA, Bennett LL, Mundie TG, Tellis CJ. Urinary desmosine excretion as a marker of lung injury in the adult respiratory distress syndrome. Chest. 1991; 100:1385–1390. [PubMed: 1935298]
55. Shen Z, Kauttu T, Seppanen H, Vainionpaa S, Ye Y, Wang S, Mustonen H, Puolakkainen P. Both macrophages and hypoxia play critical role in regulating invasion of gastric cancer in vitro. Acta Oncol. 2013; 52:852–860. [PubMed: 23193956]
56. Bell JH, Herrera AH, Li Y, Walcheck B. Role of ADAM17 in the ectodomain shedding of TNF-alpha and its receptors by neutrophils and macrophages. J Leukoc Biol. 2007; 82:173–176. [PubMed: 17510296]
57. Schaff U, Mattila PE, Simon SI, Walcheck B. Neutrophil adhesion to E-selectin under shear promotes the redistribution and co-clustering of ADAM17 and its proteolytic substrate L-selectin. J Leukoc Biol. 2008; 83:99–105. [PubMed: 17928459]
58. Gomez-Gaviro M, Dominguez-Luis M, Canchado J, Calafat J, Janssen H, Lara-Pezzi E, Fourie A, Tugores A, Valenzuela-Fernandez A, Mollinedo F, Sanchez-Madrid F, Diaz-Gonzalez F. Expression and regulation of the metalloproteinase ADAM-8 during human neutrophil pathophysiological activation and its catalytic activity on L-selectin shedding. J Immunol. 2007; 178:8053–8063. [PubMed: 17548643]
59. Hashizume M, Higuchi Y, Uchiyama Y, Mihara M. IL-6 plays an essential role in neutrophilia under inflammation. Cytokine. 2011; 54:92–99. [PubMed: 21292497]
60. Faurschou M, Borregaard N. Neutrophil granules and secretory vesicles in inflammation. Microbes Infect. 2003; 5:1317–1327. [PubMed: 14613775]
61. Gullberg U, Bengtsson N, Bulow E, Garwicz D, Lindmark A, Olsson I. Processing and targeting of granule proteins in human neutrophils. J Immunol Methods. 1999; 232:201–210. [PubMed: 10618521]
62. Mazzocca A, Coppari R, De FR, Cho JY, Libermann TA, Pinzani M, Toker A. A secreted form of ADAM9 promotes carcinoma invasion through tumor-stromal interactions. Cancer Res. 2005; 65:4728–4738. [PubMed: 15930291]
63. Millichip MI, Dallas DJ, Wu E, Dale S, McKie N. The metallo-disintegrin ADAM10 (MADM) from bovine kidney has type IV collagenase activity in vitro. Biochem Biophys Res Commun. 1998; 245:594–598. [PubMed: 9571200]
64. Hirche TO, Atkinson JJ, Bahr S, Belaaouaj A. Deficiency in neutrophil elastase does not impair neutrophil recruitment to inflamed sites. Am J Respir Cell Mol Biol. 2004; 30:576–584. [PubMed: 14565940]
65. Betsuyaku T, Shipley JM, Liu Z, Senior RM. Gelatinase B deficiency does not protect against lipopolysaccharide-induced acute lung injury. Chest. 1999; 116(1 Suppl):17S–18S. [PubMed: 10424565]

66. Higuchi Y, Yasui A, Matsuura K, Yamamoto S. CD156 transgenic mice. Different responses between inflammatory types. Pathobiology. 2002; 70:47–54. [PubMed: 12415192]

67. Bell JH, Herrera AH, Li Y, Walcheck B. Role of ADAM17 in the ectodomain shedding of TNF-alpha and its receptors by neutrophils and macrophages. J Leukoc Biol. 2007; 82:173–176. [PubMed: 17510296]

68. Tang J, Zarbock A, Gomez I, Wilson CL, Lefort CT, Stadtmann A, Bell B, Huang LC, Ley K, Raines EW. Adam17-dependent shedding limits early neutrophil influx but does not alter early monocyte recruitment to inflammatory sites. Blood. 2011; 118:786–794. [PubMed: 21628404]

69. Idell S, Thrall RS, Maunder R, Martin TR, Mclarty J, Scott M, Starcher BC. Bronchoalveolar lavage desmosine in bleomycin-induced lung injury in marmosets and patients with adult respiratory distress syndrome. Exp Lung Res. 1989; 15:739–753. [PubMed: 2478359]

70. Ricou B, Nicod L, Lacraz S, Welgus HG, Suter PM, Dayer JM. Matrix metalloproteinases and TIMP in acute respiratory distress syndrome. Am J Respir Crit Care Med. 1996; 154:346–352. [PubMed: 8756805]

71. Pardo A, Selman M. Matrix metalloproteinases and lung injury. Braz J Med Biol Res. 1996; 29:1109–1115. [PubMed: 9181053]

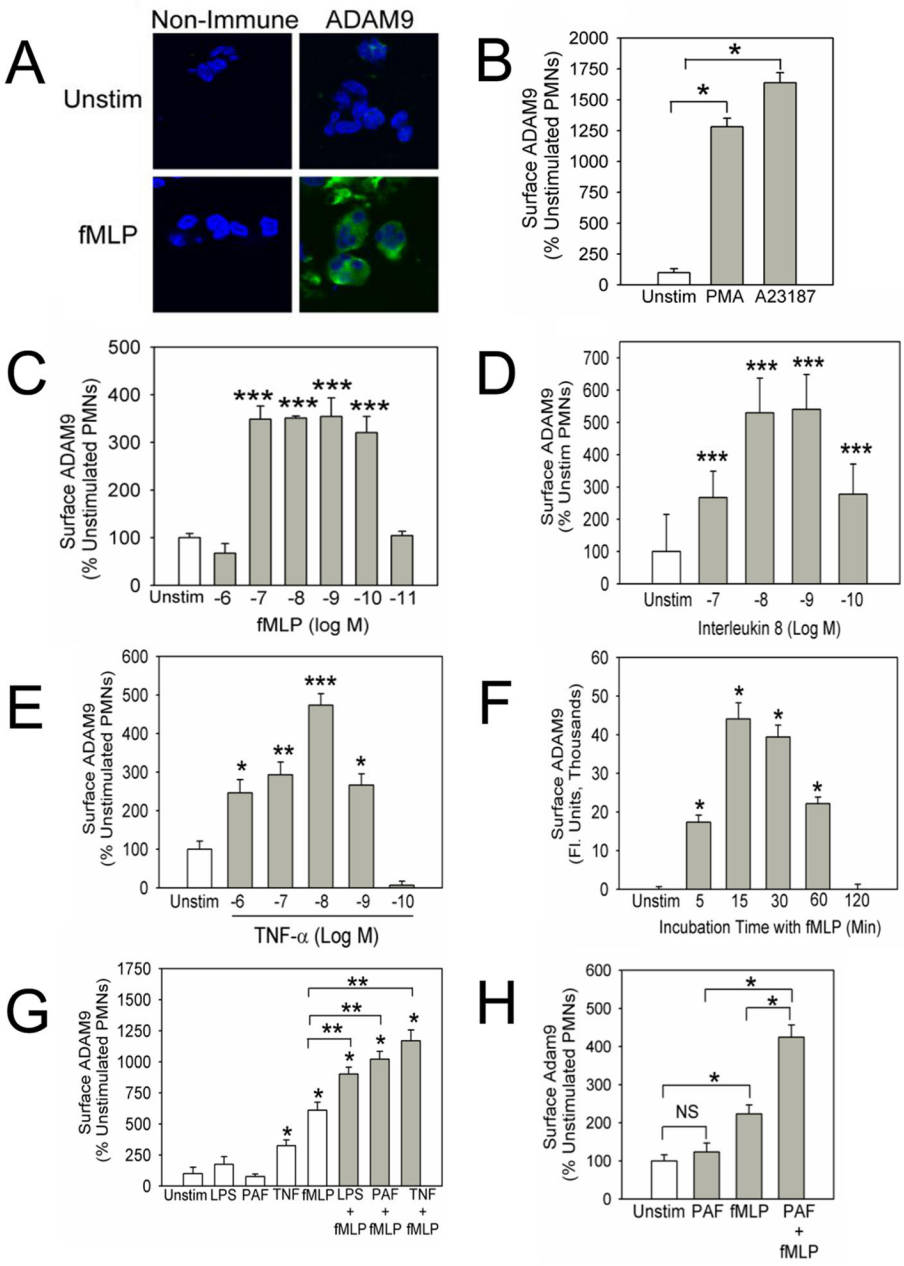

Figure 1. Pro-inflammatory mediators up-regulate surface ADAM9 levels on human and murine PMNs

In **A**, PMNs were isolated from healthy human volunteers, incubated with or without 10^{-7} M fMLP at 37°C for 30 min, and fixed. PMNs were then immunostained with Alexa-488 for surface ADAM9 or incubated with an isotype-matched non-immune primary antibody and examined using confocal microscopy. Images shown are representative of 6 separate experiments (magnification is x 400). In **B–D**, human PMNs were incubated at 37°C for 30 min with or without 10^{-7} M PMA or 10^{-6} M A23187 (**B**), 10^{-6}–10^{-11} M fMLP (**C**), 10^{-7}–10^{-10} M IL-8 (**D**), 10^{-6}–10^{-10} M TNF-α (**E**). In **F**, PMNs were incubated for up to 120 min at 37°C with or without 10^{-7} M fMLP (**F**). In **G**, PMNs were incubated for 30 min at 37°C

with or without 100 ng/ml LPS, 10^{-7} M PAF, 100 U/ml TNF-α, or 10^{-7} M fMLP alone (white bars), or PMNs were incubated at 37°C for 15 min with 100 ng/ml LPS, 10^{-7} M PAF, or 100 U/ml TNF-α and then activated for 30 min at 37°C with 10^{-7} M fMLP (grey bars). In **B–G**, cells were fixed, immunostained for surface ADAM9, and surface ADAM9 levels were quantified as described in Methods. In **B** and **F**, * indicates $p < 0.001$ versus unstimulated cells. In **C–E**, * indicates $p < 0.04$, ** $p = 0.004$, and *** $p < 0.0001$ versus unstimulated PMNs. In **G**, * indicates $p < 0.001$ compared with unstimulated cells and ** $p < 0.001$ vs. each agonist when tested alone. In **H**, PMNs were isolated from unchallenged C57BL/6 WT mice, and incubated at 37°C without agonists for 45 min (unstim), or with 10^{-6} M fMLP or 10^{-6} M PAF for 30 min, or with 10^{-6} M PAF for 15 min and then 10^{-6} M fMLP for 30 min. Cells were immunostained for surface Adam9 as described in Methods. Asterisk indicates $p < 0.001$. Data are expressed as mean ± SEM as a percentage of surface staining associated with unstimulated cells (**B–E**, and **G–H**) or in arbitrary fluorescence units (**F**); n = 150–300 cells per group. Results are representative of 3–4 separate experiments.

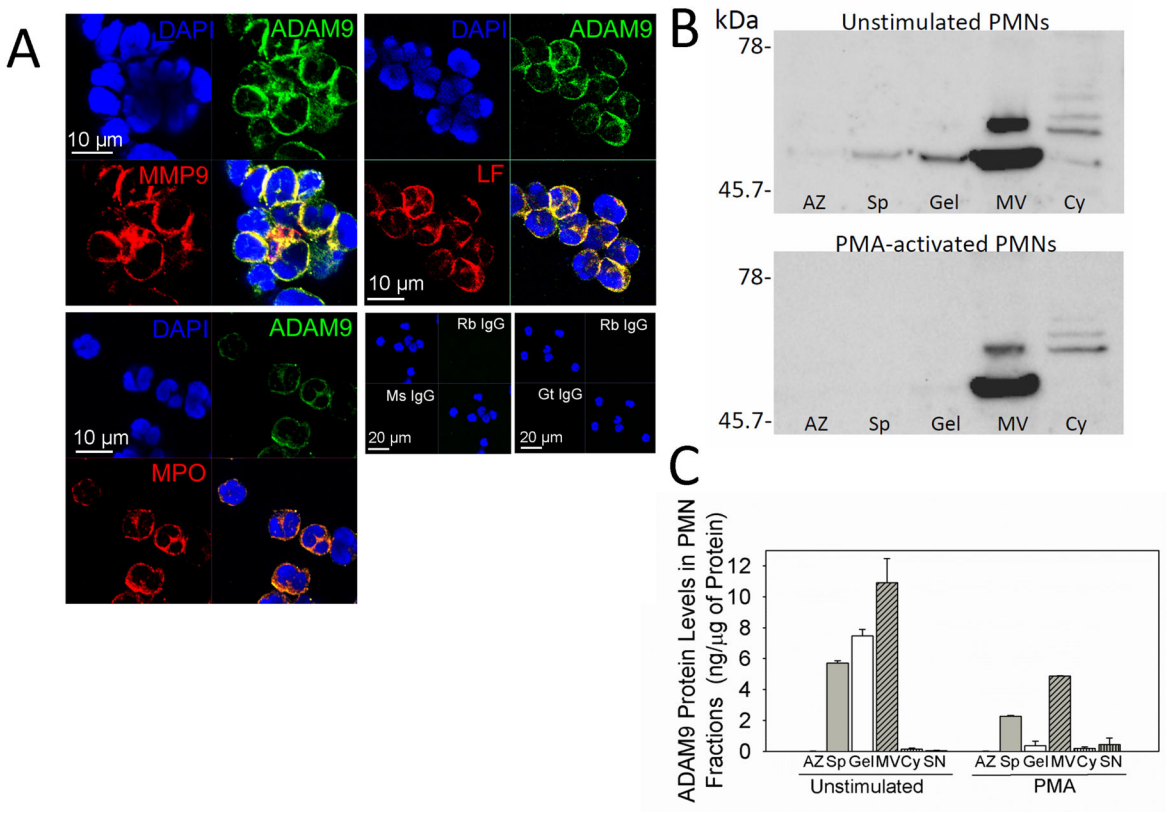

Figure 2. ADAM9 is stored in the tertiary and specific granules and secretory vesicles of PMNs

In **A**, unstimulated human PMNs were fixed, permeabilized with methanol, and then immunostained with Alexa-488 for intracellular ADAM9 (top right images) and with Alexa-546 for markers of the tertiary granules (MMP9), specific granules (lactoferrin; LF), or azurophil granules (myeloperoxidase; MPO) in the bottom left images, and nuclei were counter-stained with DAPI (top left images). Cells were examined using a confocal microscope and merged images are shown in the bottom right images. Images representative of three separate experiments are shown. As a control, PMNs were stained with isotype-matched non-immune primary antibodies [rabbit IgG (Rb IgG) and goat IgG (Gt IgG) or murine IgG (Ms IgG)] shown in the bottom right quadrant in **A**. In **B**, PMNs were incubated for 15 min at 37°C with or without PMA and then subjected to subcellular fractionation as described in Methods. The PMN granule fractions [including the azurophil (AZ), specific (Sp), and gelatinase (Gel) granules and combined plasma membrane and secretory vesicle (MV) fraction], were detergent solubilized, and along with the cytosolic fraction (Cy) subjected to western blot analysis using an antibody to ADAM9 (in **B**). ADAM9 levels were also quantified in each of these PMN fractions [and PMN supernatants (SN)] using an ELISA and results were normalized to total protein levels (**C**). Results shown in **B** are representative of PMN preparations from two donors. In **C**, data are mean ± SD (n = 2 PMN preparations).

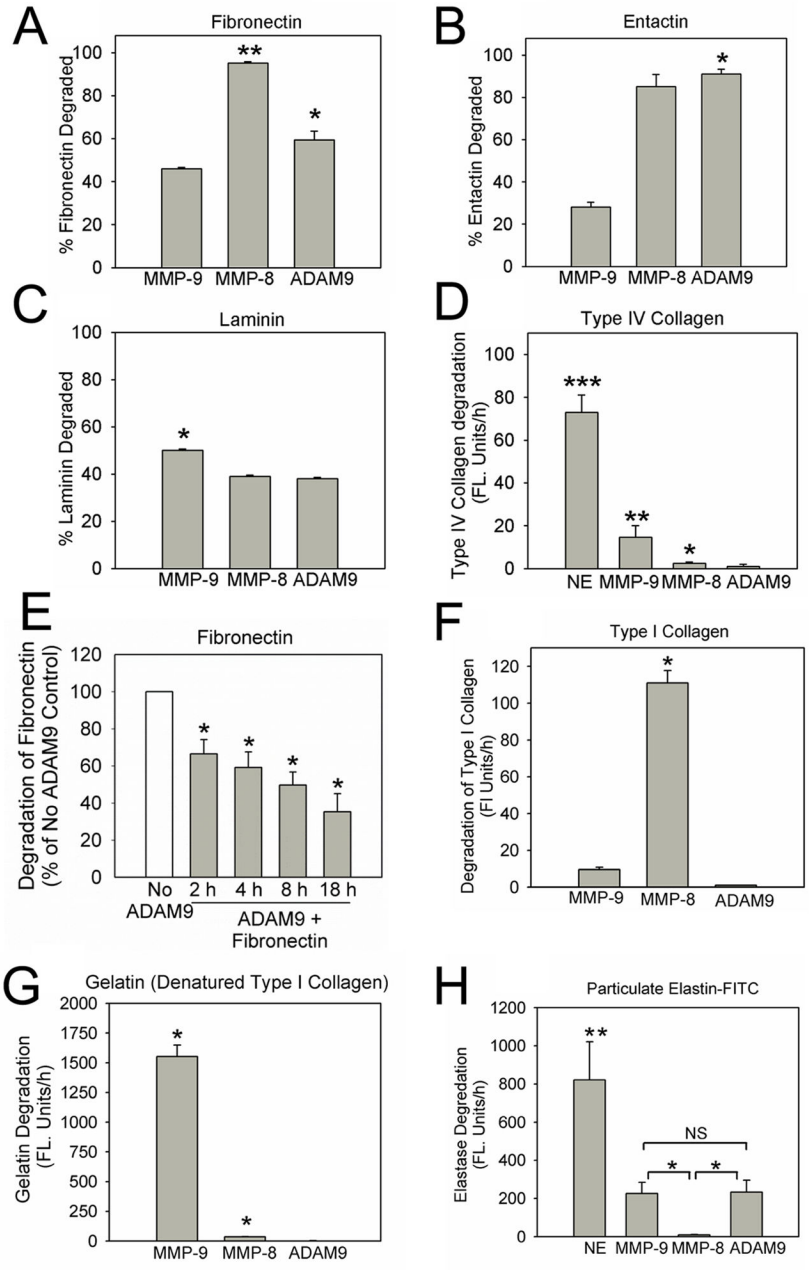

Figure 3. Soluble ADAM9 ectodomain degrades several basement membrane proteins and insoluble elastin

Equimolar (25 nM) concentrations of human soluble active ADAM9, MMP-8, or MMP-9 versus buffer alone were incubated with 2 μg of purified human fibronectin (in **A**), entactin (in **B**) or laminin (in **C**) at 37°C for 18 h at pH 7.4. The reaction products were separated on 4–20% Tris-HCl SDS-PAGE gels which were stained with Coomassie Blue dye. Densitometry was used to quantify intact ECM proteins incubated without versus with proteinases. The results are expressed as % of ECM protein that was degraded by each proteinase. Data are mean ± SEM; n = 3–6 experiments. In **A**, * indicates $p = 0.031$ and ** $p < 0.001$ versus the % of fibronectin cleaved by MMP-9. In **B**, * indicates $p < 0.001$ versus

the % of entactin degraded by MMP-9. In **C**, * indicates $p < 0.001$ versus the % of laminin that was degraded by MMP-8 and ADAM9. In **E**, 25 nM ADAM9 or buffer alone were incubated with 2 μg of fibronectin for up to 18 h at 37°C and degradation of fibronectin measured at intervals as outlined above. Data are mean ± SD (n = 4 experiments) and * indicates $p < 0.05$ versus fibronectin incubated without ADAM9. In **D, F, G,** and **H**, equimolar (25 nM) concentrations of human soluble active MMP-9, ADAM9, and MMP-8 versus buffer alone were incubated with 50 μg/ml DQ-FITC-conjugated type IV collagen (in **D**), 50 μg/ml DQ-FITC-conjugated type I collagen (in **F)**, 50 μg/ml DQ-FITC-conjugated gelatin (in **G**), or 20 mg/ml particulate elastin-FITC (in **H**) at 37°C for 18 h at pH 7.4 (in **D** and **H**, human soluble active neutrophil elastase [NE] was used as an additional control). Cleavage of each substrate was quantified in fluorescence units using fluorimetry. Results are mean ± SEM; n =3–7 experiments. In **D**, * indicates $p = 0.041$; ** $p = 0.009$; and *** $p < 0.001$ versus the amount of type IV collagen degraded by ADAM9. In **F**, * indicates $p < 0.001$ vs. the amount of type I collagen degraded by ADAM9 or MMP-9. In **G**, * indicates $p < 0.001$ vs. the amount of gelatin degraded by ADAM9. In **H**, * indicates $p = 0.033$ vs. the amounts of elastin degraded by MMP-8 and ** $p < 0.001$ vs. the amount of elastin degraded by all other proteinases.

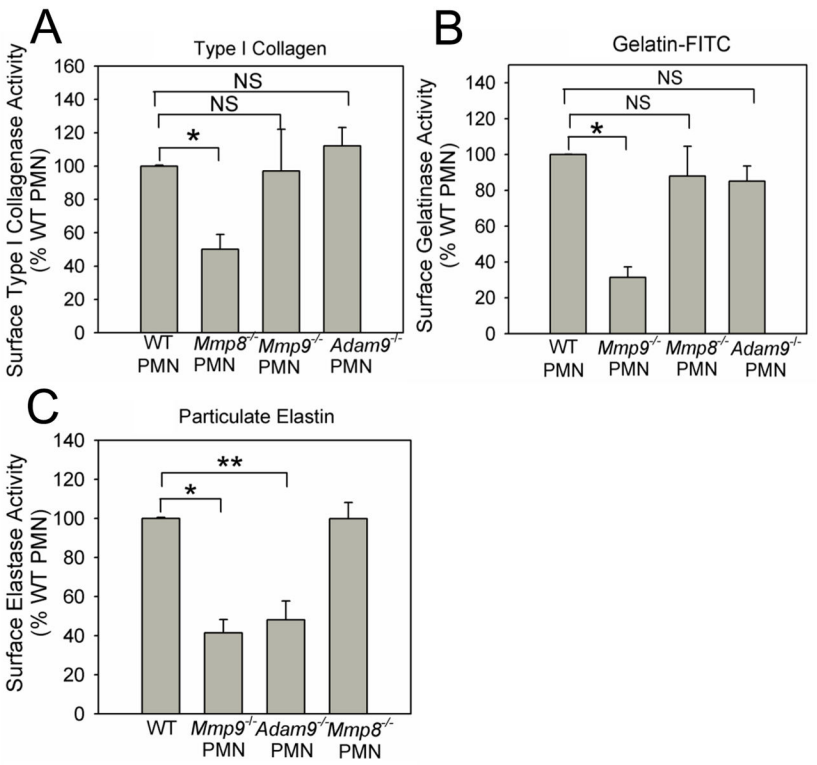

Figure 4. Surface ADAM9 on activated PMNs has similar ECM protein-degrading activity as sADAM9

We incubated equal numbers of PAF- and fMLP-activated and fixed WT, *Mmp-8*$^{-/-}$, *Mmp-9*$^{-/-}$, or *Adam-9*$^{-/-}$ PMNs versus buffer alone at 37°C for 18 h at pH 7.4 with 50 μg/ml DQ-FITC-conjugated type I collagen (in **A**), or 50 μg/ml quenched DQ-FITC-conjugated gelatin (**B**) or 20 mg/ml FITC-conjugated particulate elastin (in **C**), and quantified metalloproteinase-mediated cleavage of the substrates by surface proteinases, as described in Methods. The results for proteinase-deficient PMNs are expressed as a percentage of the MP activity associated with the surface of WT PMNs. Data are mean ± SEM; n = 3–4 experiments. In **A** * indicates p= 0.008; in **B**, * indicates $p < 0.001$; and in **C**, * indicates p = 0.006 and ** $p < 0.001$.

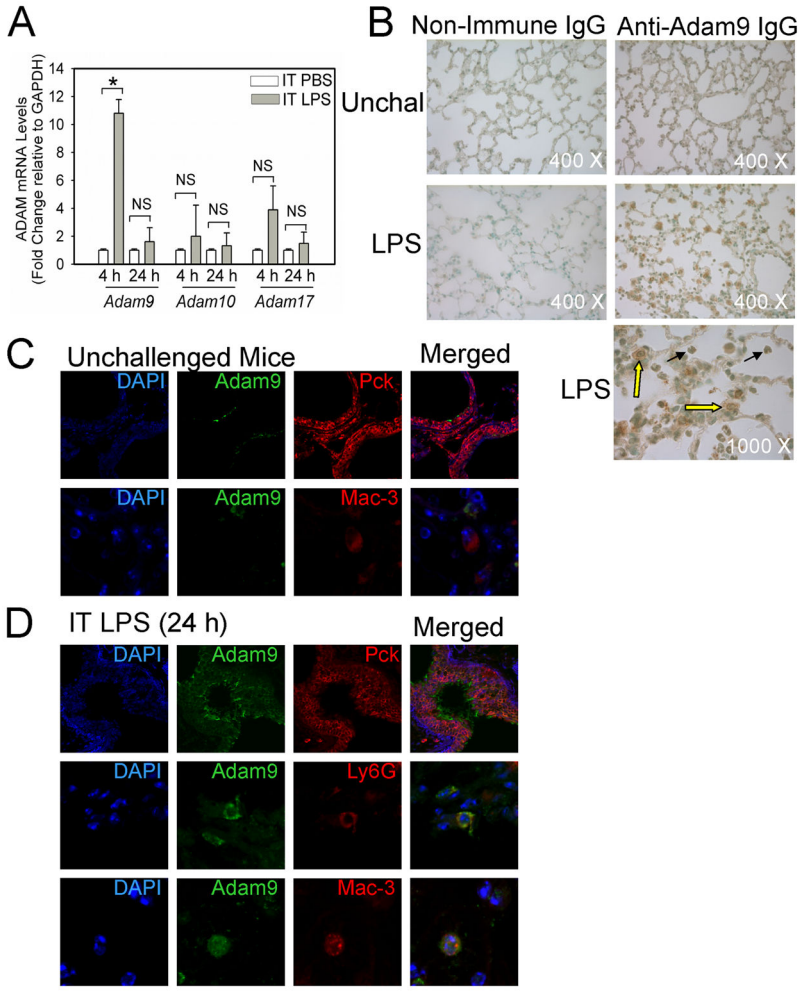

Figure 5. Adam9 is upregulated in the lung during ALI in mice

In **A**, we delivered 10 μg of LPS or PBS to C57BL/6 WT mice by the IT route, and 4 h and 24 h later measured steady state Adam9, Adam10, and Adam17 mRNA levels in whole lung samples using qRT-RT-PCR. Data are mean ± SEM; n = 6 mice/group. Asterisk indicates $p < 0.001$. In **B**, we immunostained lungs sections from unchallenged C57BL/6 WT mice (Unchal) or C57BL/6 WT mice harvested 24 h after 10 μg of LPS was delivered by the IT route using rabbit anti-Adam9 IgG or non-immune rabbit IgG and the immunoperoxidase method. Images shown are representative of 4 mice per group (magnification is x 400 and x 1000). Black arrows indicate PMNs staining positively for Adam9 and yellow arrows indicate macrophage staining positively for Adam9. In **C** and **D**, sections of lungs from unchallenged mice (in **C**) or lungs harvested 24 h after LPS was instilled by the IT route (in **D**) were immunostained with Alexa-488 for Adam9 (second columns), and Alexa-546 for markers of epithelial cells (pancytokeratin; Pck), PMNs (Ly6G), or macrophages (Mac-3). Sections were then counterstained with DAPI (first columns). Lung sections were examined using confocal microscopy, and merged images are shown in the fourth columns (magnification is X 200 for Pck-stained sections and X 500 for Ly6G and Mac3-stained sections). No staining was detected in lung sections stained with isotype matched control primary antibodies (data not shown).

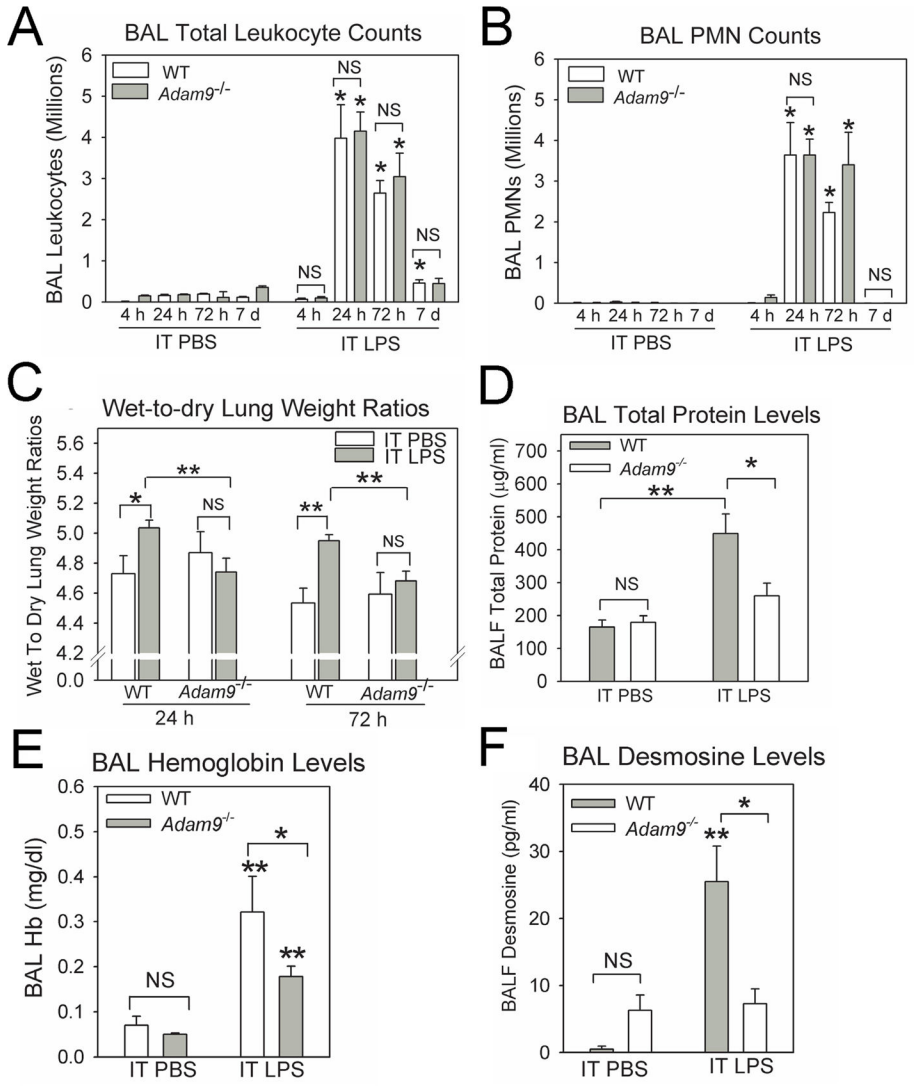

Figure 6. ADAM9 is not required for PMN recruitment into the lung but promotes LPS-mediated ALI in mice

In **A–F**, we delivered 10 µg of LPS or PBS by the IT route to WT vs. *Adam9*$^{-/-}$ mice. Four hours to 1 week later, we performed BAL or removed lungs from the mice. We counted total leukocytes (**A**) and PMNs (**B**) in BAL samples. In **A** and **B**, data are mean ± SEM; n = 5–8 PBS-treated mice and n = 15–18 LPS-treated mice. Asterisk indicates $p \leq 0.05$ compared with PBS-treated mice belonging to the same genotype at the same time point in **A** and **B**. In **C**, wet-to-dry lung weight ratios were measured 24–72 h after LPS or PBS were delivered by the IT route to WT and *Adam9*$^{-/-}$ mice. Data are mean ± SEM; n = 4–9 PBS-treated mice, n = 9–25 LPS-treated WT mice, and n = 7–16 LPS-treated *Adam9*$^{-/-}$ mice. Asterisk indicates p = 0.016 and **, $p \leq 0.002$. In **D–E**, total protein (**D**) and hemoglobin levels [in **E**, as a marker of leakage of erythrocytes across the alveolar-capillary barrier (41)] were measured in BALF samples 24 h after instilling PBS or LPS in mice. In **D–E**, data are mean ± SEM; n = 4 PBS-treated mice and n = 5–12 LPS-treated mice. In **D**, asterisk indicates $p < 0.05$ and ** p = 0.018. In **E**, asterisk indicates $p < 0.035$ and **, $p < 0.035$ versus PBS-

treated mice belonging to the same genotype. In **F**, desmosine levels were measured in BALF samples 24 h after PBS or LPS were instilled by the IT route. Data are mean ± SEM; n = 4–9 PBS-treated mice and n = 8–16 LPS-treated mice. Asterisk indicates p = 0.016 and ** p = 0.021 versus PBS-treated WT mice.

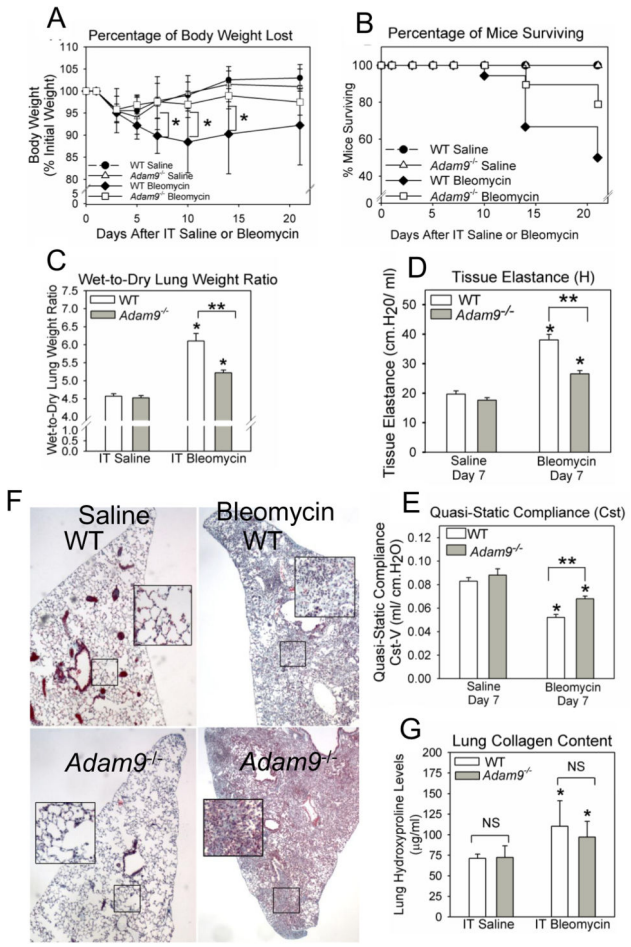

Figure 7. ADAM9 promotes weight loss, mortality, and ALI but does not regulate lung collagen accumulation in bleomycin-treated mice

In **A–B**, we delivered 30 mU of bleomycin vs. saline by the IT route to WT vs. *Adam9*$^{-/-}$ mice and measured changes in body weight relative to baseline body weight (**A**) and recorded survival of the mice (**B**) over 21 days. In **A**, n = 4–5 saline-treated mice and n = 22 bleomycin-treated mice were studied. Asterisk indicates $p \leq 0.044$ for bleomycin-treated WT versus bleomycin-treated *Adam9*$^{-/-}$ mice. In **B**, n = 5–8 saline-treated mice and n = 9–15 bleomycin-treated mice were studied. In **C–E**, we delivered 100 mU of bleomycin vs. saline by the IT route to WT vs. *Adam9*$^{-/-}$ mice and measured wet-to-dry lung weight ratios and respiratory mechanics using a FlexiVent device. In **C**, 7–17 saline-treated mice and 8–10 bleomycin-treated mice were studied per group. Asterisk indicates $p < 0.001$ when compared with saline-treated mice belonging to the same genotype and ** indicates $p < 0.001$. In **D–E**, 4–6 saline-treated mice and 5–9 bleomycin-treated mice were studied per group. Asterisk indicates $p < 0.001$ for saline-treated mice belonging to the same genotype and ** indicates $p < 0.001$. In **F–G**, 30 mU of bleomycin or saline was instilled by the IT route to WT vs. *Adam9*$^{-/-}$ mice and 21 days later, the right lungs were inflated, removed, fixed, and stained with Masson's trichrome stain. Representative images of lung sections from saline- and bleomycin-treated WT and *Adam9*$^{-/-}$ mice are shown in **F** (magnification is X100 and magnification of insets is x 400). In **G**, lung collagen levels were assessed using

hydroxyproline assays performed on hydrolysates of left lungs removed after 21 days. In **G**, data are mean ± SEM; n = 5 saline-treated mice and n = 9–15 bleomycin-treated mice. Asterisk indicates $p \leq 0.043$ when compared with saline-treated mice belonging to the same genotype.

Table I

ADAM9 Protein Levels in PMN Extracts and Release of sADAM9 from Unstimulated and Activated PMNs

Experimental condition //	ADAM9 Protein Levels in PMN Cell Extracts (pg/10^6 PMNs)	sADAM9 released by PMNs (% of amount contained within unstimulated PMNs)**
Unstimulated	65.6 ± 10.3#	4.7 ± 2.5%
TNF-α	59.0 ± 11.5	4.6 ± 1.8%
PAF	64.8 ± 12.2	4.1 ± 2.4%
fMLP	49.4 ± 8.9	4.2 ± 2.4%
TNF-α + fMLP	59.1 ± 6.5	4.3 ± 2.0%
PAF + fMLP	60.9 ± 9.8	5.3 ± 2.3%

// PMNs isolated from healthy human donors were incubated at 37°C for 30 min with or without 100 U/ml TNF-α, 10^{-7} M PAF, or 10^{-7} M fMLP. PMNs were also primed for 15 min with 100 U/ml TNF-α or 10^{-7} M PAF, and then activated for 30 min with 10^{-7}M fMLP (TNF-α + fMLP and PAF + fMLP). Cells and cell-free supernatant fluids were separated by centrifugation, and ADAM9 protein levels were measured in cell extracts and cell-free supernatant fluids using an ELISA.

Data are mean ± SEM; n = 4 donors.

** Results for amounts of sADAM9 released by PMNs are expressed as a percentage of the cellular content of ADAM9 in extracts of unstimulated PMNs.

There are no significant differences in the amounts of ADAM9 quantified in extracts of unstimulated vs. activated PMNs, or in the amount of sADAM9 released by unstimulated vs. activated PMNs.

Table II

Activation of PMNs with fMLP for up to 4 h does not alter ADAM9 protein levels in cell extracts or cell-free supernatant fluids

Experimental Condition[#]	ADAM9 Protein Levels in PMN Cell Extracts (pg/10^6 PMNs)	sADAM9 released by PMNs (% of amount contained within unstimulated PMNs)
unstimulated	65.48 ± 7.84[§§]	3.2 ± 1.5%
fMLP 1 h	73.67 ± 6.57	4.8 ± 2.7%
fMLP 2 h	49.77 ± 12.10	3.9 ± 1.2%
fMLP 4 h	59.18 ± 13.70	5.2 ± 1.6%

[#]PMNs were isolated from healthy human donors and an extract of freshly isolated cells was prepared (unstimulated). Other aliquots of PMNs were incubated at 37°C for 1–4 h with 10^{-7} M fMLP. Cell-free supernatant samples were removed, and cell extracts prepared. ADAM9 protein levels were quantified in PMN extracts and cell-free supernatant fluids using an ELISA. Data for sAdam9 amounts released by PMNs are expressed as a percentage of the amount of ADAM9 protein measured in extracts of unstimulated cells from the same donor.

[§§]Data are mean ± SEM; n = 4 donors.

There are no significant differences in the amounts of ADAM9 quantified in extracts of unstimulated versus fMLP-activated PMNs, or in the amount of sADAM9 released by unstimulated versus fMLP-activated PMNs.